

It is my pleasure to review the manuscript "The incorporation of an organic soil layer in the Noah-MP Land Surface Model and its evaluation over a Boreal Aspen Forest" by Chen et al.

The authors incorporated an organic soil layer into Noah-MP and evaluated its performance over a Boreal Aspen Forest site. The method is straightforward, however part of the results and conclusions are questionable due to the unrealistic simulations of liquid water and ice during the cold season. Besides, there are a couple of flaws or misleading expressions. According to this, a major revision is suggested, and the authors are encouraged to substantially revise the manuscript and re-submit it.

*Thank you for your thoughtful comments, which are very helpful in improving the presentation and scientific content of the manuscript. We have carefully taken them into account when revising the manuscript, and our response below is in italic.*

My major concerns are as follows:

- 1) In Figure 5, the liquid water in the top soil layer is much underestimated or unrealistically simulated comparing to the observation after incorporating the organic soil layer. In Figures 8&9 as well as Sections 4.3&4.4, the authors show that the inclusion of organic soil layer produces comparable or worse simulations of turbulent heat flux during summer, autumn and winter compared to the default model setting, and only improvement is seen in spring. Since the water and heat is strongly coupled during cold season including spring, the underestimation of liquid water or overestimation of ice in the top soil layer during cold season will inevitably affect the simulations of turbulent heat flux. Hence, if the underestimation of liquid water in the top soil layer during cold season cannot be resolved appropriately, the conclusion drawn upon this is questionable.

*In the previous revision, we only applied the parameters recommended by Lawrence et al. (2008), which assumed the soil as fibric peat and larger porosity and smaller  $b$ . However, for our specific site, the measured soil-bulk density is about  $160 \text{ kg m}^{-3}$ , and the soil should be defined as hemic peat, a medium humified organic soil. We believe the bias in the OGN simulation shown in last revision was mainly because of the inappropriate assumption of the soil parameters. Therefore, we redefined the organic soil for this site as hemic peat, used more appropriate soil parameters for the OGN simulation, and conducted more sensitive tests.*

*In cold season when the soil is frozen, the soil moisture measurements are questionable and should be treated with cautious. In summer, the soil moisture in the new OGN simulation is improved, and results also show improved the soil temperature. Although the simulated SH and LH by CTL are very similar to OGN for drought years, in wet years the fluxes are improved significantly in spring. For summer, autumn and winter, the OGN simulation is slightly worse than CTL, but their differences are very small.*

*The other factor complicating the model evaluation is the closure problem in the observed surface energy budget. Barr et al. (2012) calculated the energy closure for this site, showing that the ratios of  $SH + LH$  to  $RN - G$  ( $EBR = (SH + LH) / (RN - G)$ ), integrated over 10 hydrologic years (1999-2009), were 0.81. This means that the  $SH + LH$  were underestimated for about 19% compared with the value of  $RN - G$ .*

*Barr et al. (2006) also gave evidence that the measured and "missing" fluxes may have different Bowen ratios, based on the data from the deciduous Old Aspen site (OAS) in this study. The EBR at OAS varied seasonally, with higher EBR during leafless periods when the*

*Bowen ratio was high and lower EBR during fully leafed periods when the Bowen ratio was low. It is impossible to estimate the flux partition for the deficit between SH and LH.*

- 2) The underestimation of liquid water in the top soil layer is due to the introduction of much lower value of b parameter for the organic soil (see Table 2). The values suggested by Lawrence and Slater (2008) are directly adopted in this study for the organic soil layer. The authors also did a sensitivity test and showed that the total water contents are not sensitive to the specific soil parameters. However, the chosen of parameter ranges, 4 times for hydraulic conductivity and 5-20% for other parameters, is not rigorous, since Letts et al. (2000) showed that the value for b parameter of organic soil ranges between 2.7 and 12, and for hydraulic conductivity ranges between  $0.1$  and  $280 \times 10^{-6}$  m/s. Besides, it's better to show how the parameters affect the soil moisture simulation of each layer.

*We conducted additional sensitivity tests followed the method of Letts et al. (2000). The organic soil is in the top layer for our study site and originally set as fibric peat in our last version. The parameter values for fibric peat were shown in Table 2 in the previous version (based on Letts et al. 2000). As mentioned in the above response, the soil at OAS site should be defined as hemic peat, a median organic soil. Based on this, we set the range of the parameters for our sensitivity test to cover all the possible values. We compared the sensitivity test simulation results for each layer. For hydraulic conductivity, the organic soil is much higher than the mineral soil, the hydraulic conductivity of organic soil ranges between  $0.1$  and  $280 \times 10^{-6}$  m/s. If the first layer organic soil is hemic peat, the recommended hydraulic conductivity is around  $2 \times 10^{-6}$  m/s. Figure A shows that the summer soil water content of the first layer became higher (lower) when the value of hydraulic conductivity decreases (increases), but the winter values did not change. For porosity (Figure B), the soil water content of the first layer became lower (higher) when the value of porosity decreases (increases).*

*However, the b parameter mainly influences the winter soil moisture, and it is recommended to use 6.1 for hemic peat. Figure C shows that using the value of 6.1 improved the simulated winter soil water content. While the simulated summer values are not sensitive to the b parameter. Little changes are shown for the deeper soil layers, with more significant differences in cold season when the soil is frozen.*

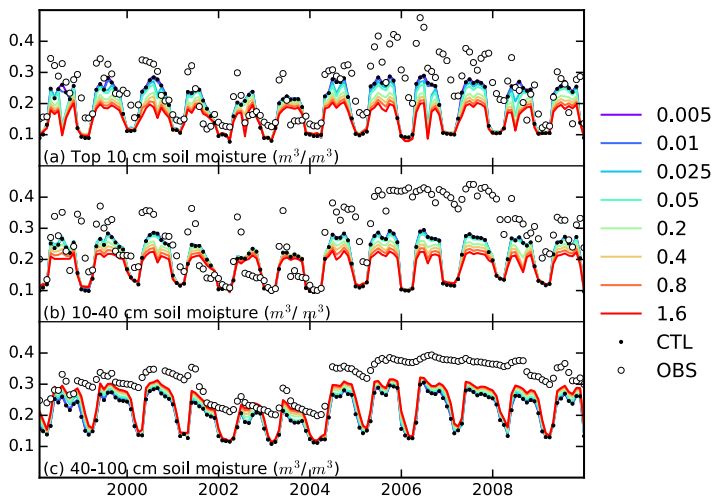


Figure A: Sensitivity test of soil liquid water content to varying hydraulic conductivity (Unit:  $m\ s^{-1} \times 10^{-3}$ ).

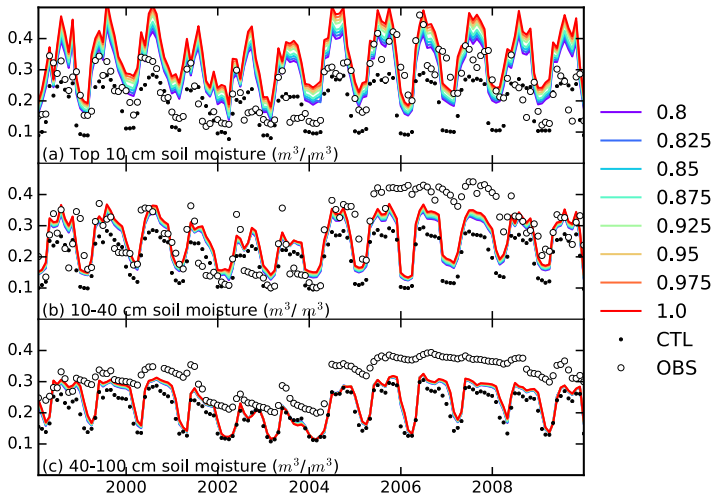


Figure B: Sensitivity test of soil liquid water content to varying porosity.

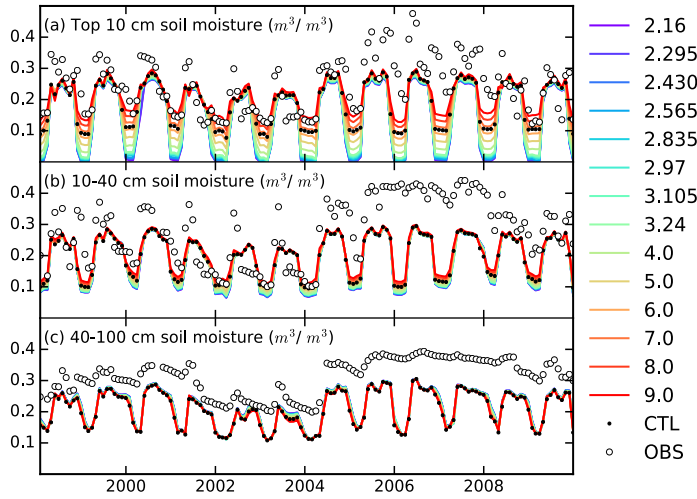


Figure C: Sensitivity test of soil liquid water content to varying  $b$ .

- 3) Since a pure organic soil layer is assumed, the parameterization of organic soil in this paper is not exactly the same as the parameterization proposed by Lawrence and Slater (2008) as well as the Equations (1) and (2) shown in section 3.1. It's suggested to remove the equations and rewrite the method. The method adopted here is straightforward, and it's suggested to collect the soil samples and measure the hydraulic and thermal properties of organic soil directly, which will largely overcome the parameter uncertainties.

*The measurement of the soil properties for this site conducted by Barr et al (2006) shows that the soil is an Orthic Gray Luvisol (Canadian Soil Classification System) with an 8-10 cm deep forest-floor (LFH) organic horizon overlying a loam Ae horizon (0-21 cm), a sandy clay loam Bt horizon (21-69 cm), and a sandy clay loam Ck horizon (69+ cm).*

*The Noah-MP model has 4 soil layers, the thickness of the top layer is 10 cm, and the thickness of the second layer is 30 cm (10-40cm). To ensure that the soil layer setup is close to the ground truth, we set the first layer as a pure organic soil. The second layer is considered as a transition layer, and we set the fraction of organic soil to be 30% instead. As to the third and fourth layers, the organic soil fractions are set to 0.*

*So based on this modification, we revised the sentences to read as "In this study, we assume that the top-soil layer is made up of 100% organic matter, consistent with the 8-10 cm LFH horizon at OAS, with the carbon fraction equals to 1. The soil properties for this layer are calculated based on the parameters of organic soil. The second layer of the soil is considered as transition layer and made up of 30% organic matter with the carbon fraction equals to 0.3. The soil properties for this layer are specified as a weighted combination of organic and mineral soil properties:"*

$$P = (1 - f_{sc,i})P_m + f_{sc,i}P_o$$

*where  $P_m$  is the value for mineral soil,  $P_o$  is the value for organic soil, and  $P$  is the weighted*

*average quantity. The remaining soil layers were assumed to be 100% mineral soil, the carbon fraction equals 0, the soil properties for this layer are calculated based on the parameters of mineral soil.”*

- 4) Another uncertainty with the introduction of organic soil layer is that it will cause the discontinuity of soil moisture between the first and second soil layers. Specifically, the soil water potential between the interface of first and second soil layers is identical or continuity. However, due to the different soil parameters assigned for the first and second soil layers, which will cause different soil moisture for layer interface with the identical soil water potential. The authors are suggested to address this problem appropriately and to show how will this affect the soil moisture simulation results.

*The water flux is continuous across the boundary between two soil layers, as the liquid water flow occurs in response to a hydraulic potential gradient but not necessarily in response to a water content gradient. So the water potential is continuous, as well as the matric potential and the matric head. Since the soil water characteristic is in general different for two different layers, the water content is in general discontinuous.*

*The hydraulic properties for organic soil and mineral soil are very different as can be seen in Table 2 in the manuscript. The saturated hydraulic conductivity of the organic soil (hemie peat) is slightly lower than that of the mineral soil (sandy clay loam), but the hydraulic conductivity is a soil property that is highly dependent on the soil water content, which may decrease several orders of magnitude as the water content changes from saturation to permanent wilting. The saturated matric potential for organic soil is much lower than that of the mineral soil,*

*In this study, the organic soil fraction of the first layer was set to 100%, while in the second layer the organic soil fraction was set to 30% as a transition layer. We conducted several sensitive tests to find out the impact of parameter uncertainties on simulated soil moisture, similar to what we did to address the major comment #2. Results show that the simulated top-layer soil moisture is very sensitive to the soil porosity, saturated hydraulic conductivity, saturated matric potential, and Clapp and Hornberger parameter. For the topsoil layer, the OGN parameterization increases the liquid soil water content in summer as water fills the larger pores of organic soil, though the liquid soil water content in winter didn't change much. Clearly, the soil liquid water content is mainly controlled by precipitation, soil hydraulic conductivity, and runoff. Higher porosity of organic soil in the topsoil layer helps retain more snowmelt water and hence increases the topsoil layer liquid water content. For the deep soil layers, the soil liquid water content is highly influenced by freeze-thaw cycle and increases during soil ice thawing period. The higher deep soil layer liquid water content in OGN is mainly caused by its higher soil hydraulic conductivity and by more liquid water in the top two soil layers for OGN, because the latter can be transported downward quickly into the deeper layers. Although the organic soil layer is only added to the top two layers in this study, it still can indirectly affect the deep layer due to the increased infiltration in the topsoil.*

*The results from the designed simulations (Figure E) show that a shallow layer of the topsoil is always dry, due to higher hydraulic conductivity of organic soil, which is consistent with the conclusion in Lawrence et al., (2008).*

*This study site has a typical two-layer soil with organic soil overlying mineral soil, but the transition between organic and mineral soil layers is often rather sharp. This kind of discontinuity in soil water between different layers exists in the real soil. As shown in Figure G, the 10cm interface in OGN\_1 and the 40cm interface in aOGN\_2 the 40 have obvious discontinuity in vertical soil water profile in spring (Figure G). This is because the different soil type leads to different soil water. Such distinct layers of soil texture exist in the real soil (personal communication with Dave Gochis). But this discontinuity is much reduced in the summer season (Figure F), so it does not significantly affect the discussions of summer results in this paper.*

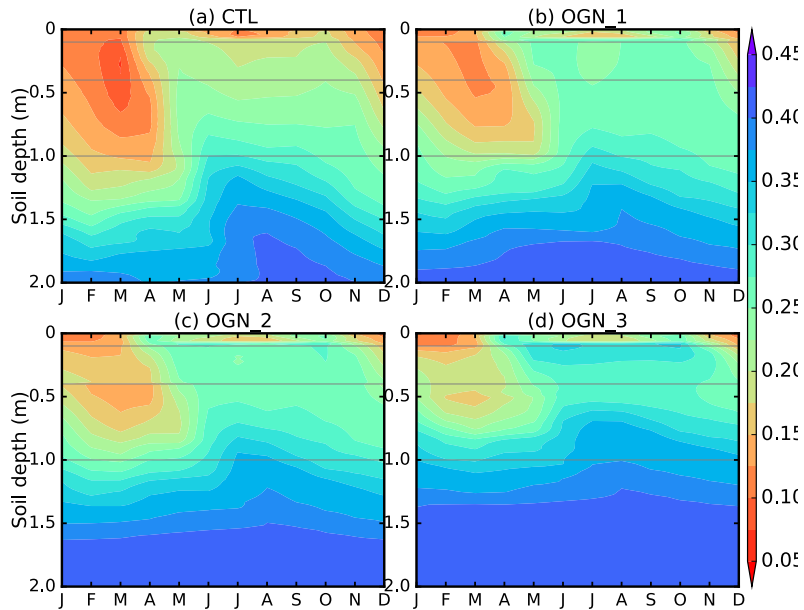


*Figure E: Four additional simulations with 100 soil layers for multi-year monthly climatology (1998-2009), and the thickness of each soil layer is 2 cm. (a) without organic soil, equivalent to the control run (CTL); (b) with the top 5 soil layers (0~10 cm) to be 100% organic soil, and the rest (6-100) layers are mineral soils, equivalent to the old OGN run (OGN\_1); (c) top 5 soil layers (0~10cm) are 100% organic soil, 6~20 soil layers (10~40cm) are fractional (30%) organic soil as a transition layer, and the rest (21-100) layers are mineral soil, equivalent to the new OGN run in this version (OGN\_2); and (d) top 5 soil layers (0~10cm) are 100% organic soil, layer 6 to 25 (10~50cm) are organic soil in which the fraction of organic soil decreases by 5% for each layer, i.e., layer 6 has 100% organic soil, while layer 7 has 95% organic soil, and so forth, and the 25<sup>th</sup> layer has 0% organic soil. This makes the vertical transition of the soil characteristic more gradually (OGN\_3).*

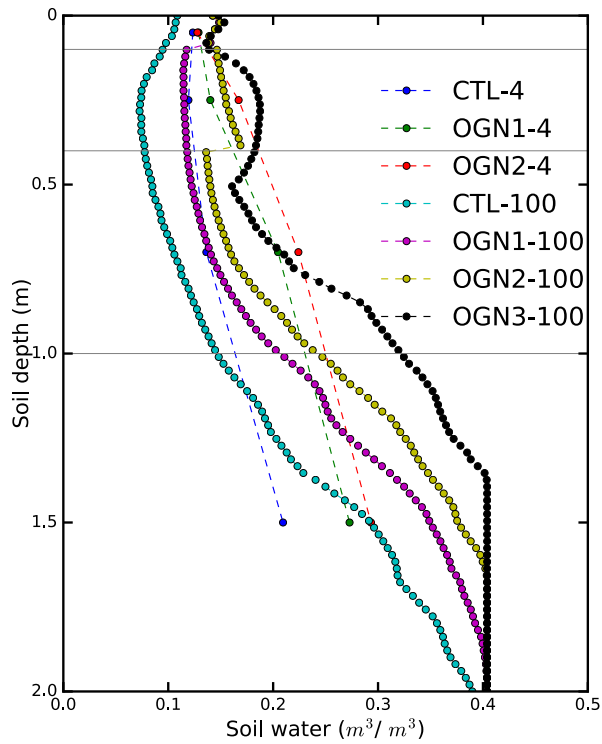


Figure F: The vertical profile of the soil water in March for multi-year monthly climatology (1998-2009), CTL\_4 denotes the control run with 4 soil layers; OGN1\_4 denotes 4 soil layers with the top soil layers (0~10 cm) to be 100% organic soil, and the rest layers are only mineral soil, OGN2\_4 denotes 4 soil layers with the top soil layers (0~10 cm) to be 100% organic soil, and the second soil layers (10~40cm) are fractional (30%) organic soil as a transition layer, and the rest layers are only mineral soil, the CTL\_100, OGN1\_100, OGN2\_100 and OGN3\_100 are the same as described in Figure E.

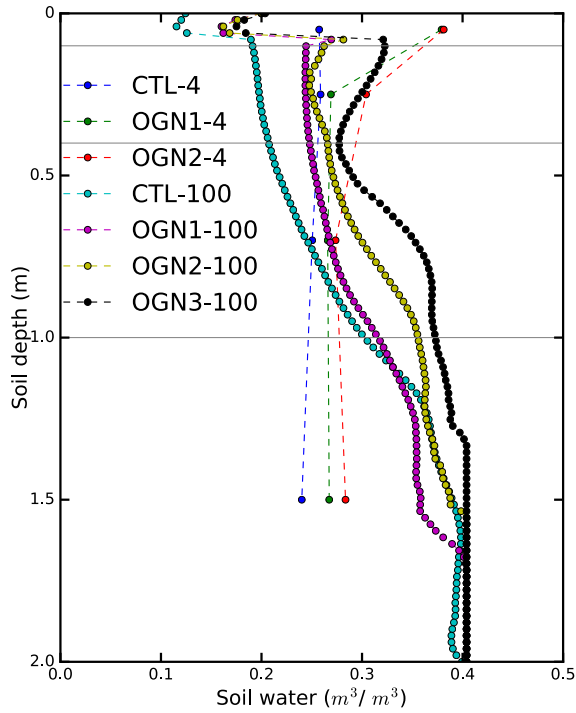


Figure G: the vertical profile of soil water in July for multi-year monthly climatology (1998-2009), CTL\_4 denotes the control run with 4 soil layers; OGN1\_4 denotes 4 soil layers with the top soil layers (0~10 cm) to be 100% organic soil, and the rest layers are only mineral soil, OGN2\_4 denotes 4 soil layers with the top soil layers (0~10 cm) to be 100% organic soil, and the second soil layers (10~40cm) are fractional (30%) organic soil as a transition layer, and the rest layers are only mineral soil, the CTL\_100, OGN1\_100, OGN2\_100 and OGN3\_100 are the same as described in Figure E.

- 5) In section 4.4, Line 328-337, the authors attribute that the overestimation of sensible heat flux during summer time is due to the energy imbalance in observations. If it's the case, the authors are suggested to address the energy closure problem appropriately, and then compare the model simulation with the correct observations, which may subsequently change the results presented in Table 3, Figures 6-12 and the corresponding text.

The seasonal changes of EBR are shown in Figure H. On average, the daily averaged SH+LH were lower than the daily averaged RN-G (so EBR is always smaller than 1), with

daytime-averaged value lower than daily-averaged value (indicating that nighttime observations are not so reliable), and noisier for winter. Barr et al. (2012) calculated the energy closure for this site in warm season, and showed that the EBR over 10 hydrologic years (1999-2009) was 0.81. In our calculation (Figure D) the daily and daytime EBR are within the reported range (e.g., Twine et al., 2000; Wilson et al., 2002; Tanaka et al., 2008; Barr et al., 2006). To represent uncertainties in observed fluxes, we added error bars on the observed SH & LH in Fig. 6 (shown below as Figure I). These also help explain the annual cycle of SH in Figs 7, 10, 11 in which both OGN and CTL simulated SH are higher than observations, and similar patterns are found for the diurnal cycle of SH & LH (Figs 8 & 9). Given the surface energy unbalance in observations and the observed SH is underestimated, OGN simulated SH may in fact be closer to the truth.

*References:*

Barr, A G, Kai Morgenstern, T A Black, J H McCaughey, and Zoran Nestic. "Surface Energy Balance Closure by the Eddy-covariance Method Above Three Boreal Forest Stands and Implications for the Measurement of the CO<sub>2</sub> Flux." *Agricultural and Forest Meteorology* 140, no. 1 (2006): 322-337.

Barr, A G, G Van der Kamp, T A Black, J H McCaughey, and Z Nestic. "Energy Balance Closure at the BERMS Flux Towers in Relation to the Water Balance of the White Gull Creek Watershed 1999--2009." *Agricultural and Forest Meteorology* 153 (2012): 3-13.

Twine, Tracy E., W. P. Kustas, J. M. Norman, D. R. Cook, PRea Houser, T. P. Meyers, J. H. Prueger, P. J. Starks, and M. L. Wesely. "Correcting eddy-covariance flux underestimates over a grassland." *Agricultural and Forest Meteorology* 103, no. 3 (2000): 279-300.

Wilson, Kell, Allen Goldstein, Eva Falge, Marc Aubinet, Dennis Baldocchi, Paul Berbigier, Christian Bernhofer et al. "Energy balance closure at FLUXNET sites." *Agricultural and Forest Meteorology* 113, no. 1 (2002): 223-243.

Tanaka, Hiroki, Tetsuya Hiyama, Nakako Kobayashi, Hironori Yabuki, Yoshiyuki Ishii, Roman V. Desyatkin, Trofim C. Maximov, and Takeshi Ohta. "Energy balance and its closure over a young larch forest in eastern Siberia." *agricultural and forest meteorology* 148, no. 12 (2008): 1954-1967.

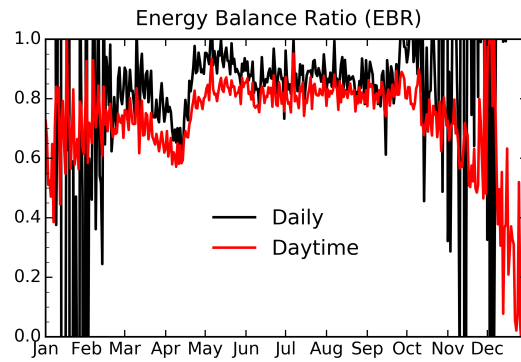


Figure H: Daily and daytime energy balance Ration ( $EBR=(SH+LH)/(RN-G)$ )

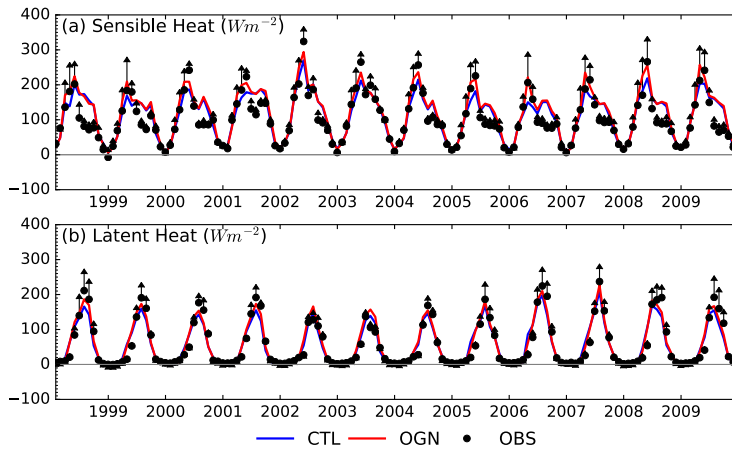


Figure I. Observed and the Noah-MP simulated (CTL and OGN) monthly sensible and latent heat flux above tree canopy, the error bars represent the average and deviations  $[(RN-G) \times B / (1+B)]$  for SH, and  $(RN-G) / (1+B)$  for LH] from observations.

The minor concerns are as follows:

- 1) Line 228-230, “Lower (higher)...to CTL”. This expression here is nor rigorous, since more ice is produced during winter, which will increase the thermal heat conductivity.

*Agree. The original text is not clear and now revised to read “In summer, dues to lower saturated thermal conductivity (0.25 W/m K for organic compared to ~6.04 W/m K for mineral) in OGN, the downward transfer of hear from topsoil layer is less and the deep soil temperature in OGN is lower than that in CTL. In winter, with the presence of soil ice, the thermal heat conductivity in OGN (~2.20 W/m K) is lower than that in CTL (6.04 W/m K), it reduces the upward transfer of heat from deep soils to topsoil and therefore results in higher*

*deep-soil temperature in OGN.”*

- 2) Line 310-320, “OGN has...sensible heat flux”. This part is lack of context with the previous presentation and also there are not figures or tables to support the text. Since this section is focused on the diurnal cycle, maybe it is better to remove this part or move it to section 4.5.

*Lines 444-453: This part has been moved to section 4.5.*

- 3) Line 331, the term “GFX” is not defined before.

*Line 396: Changed the GFX to G as ground heat flux.*

- 4) Line 340, change “last” to “previous”.

*Line 404: Revised “last” to “previous”*

- 5) As shown in table 1, the authors choose the zero heat flux as the soil temp lower boundary. Since the soil column is 2m, which maybe too shallow to configure with the zero heat flux to correctly simulate the multi-year soil temperature dynamic over the frozen soil/permafrost area. Can the authors comment on this?

*We agree with the reviewer that the zero heat flux applied for a 2-m soil column in this study may not appropriate. To assess this, we tried the other option: to set TBOT at 8m with annual-mean 2m air temperature as the lower boundary condition for soil temperature. We compared the zero-heat-flux simulation and the TBOT simulation (Figure J), and found that the soil temperature in the deep soil layers is difference, mainly in autumn and winter. The TBOT simulated soil temperature in 3rd and 4th layers became lower than the zero-heat-flux simulation and there are closer to the observation. Therefore, we used TBOT boundary conditions in this study, and revised all the results in this paper including all the figures and tables.*

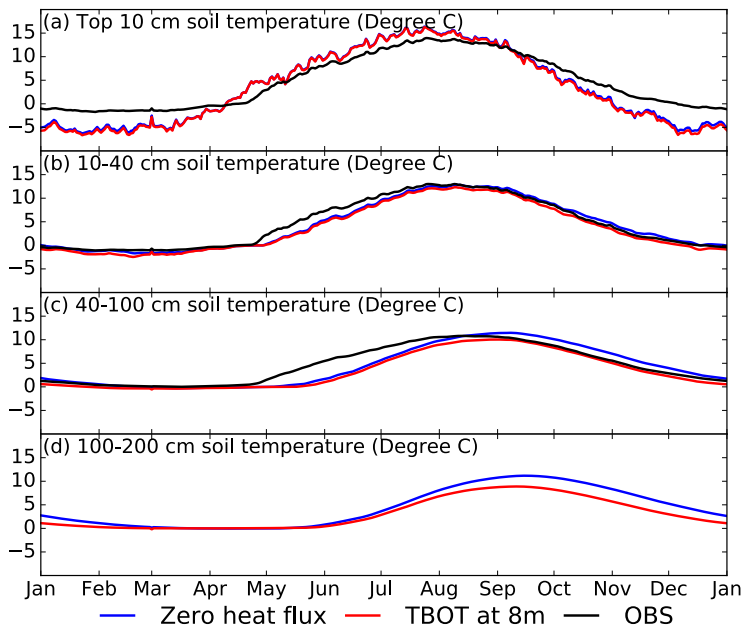


Figure J: Comparison of the annual cycle of the simulated soil temperature between Zero heat flux and TBOT at 8m.

- 6) The authors describe in Line 410-411 that they plan to apply the parameterization proposed in this paper to other region, the question here is that is it the parameters adopted in this paper also applicable to other region, or what's the challenge to transfer the parameter or address the parameter uncertainty?

*This article shows tremendous model sensitivity to soil organic properties. The future challenge of applying this parameterization to regional and global scales is to properly define the vertical structures of organic-soil fraction and properties. That would need to develop spatial maps of organic soil content, and rely on soil observationists to define robust relationships between organic soil content and various soil thermal and hydraulic parameters*

Title: The incorporation of an organic soil layer in the Noah-MP Land Surface Model and its evaluation over a Boreal Aspen Forest

Authors: Liang Chen et al.

The authors have responded adequately to the reviewer comments on the manuscript.

*Thank you for your thoughtful comments, which are very helpful in improving the presentation and scientific content of the manuscript. We have carefully taken them into account when revising the manuscript, and our response below is in italic.*

General comments: I suggest that the authors should review the text (e.g., phrases construction), especially in the abstract and results.

A few minor comments to address:

- Line 145: Lack includes the subscript in the term  $f$  of the equation.

*This is a mistake. The text has been change to reflect  $f_{sc,i}$ , the carbon fraction of the each layer.*

- Lines 209 and 210: only CTL simulation? I understood that the authors analyzed together CTL and OGN simulations and observations.

*Revised the sentence to read as “We first evaluated the CTL and OGN simulated soil temperature and moisture at the OAS site in relation to observations for the period of 1998-2009.”*

- In a few sentences the authors do not specify the object of comparison. For example:

Lines 215-218: “However, for deep layers (10-100cm), the OGN simulated much lower (higher) soil temperatures during summer (winter), especially for the drought years 2002-2003, leading to a good agreement between OGN and observations for 2<sup>nd</sup> and 3<sup>rd</sup> layer soil temperature (Figure 4b, c).”

Higher and lower than ....

I would replace the above sentence by “However, for deep layers (10-100cm), soil temperature from the OGN is lower (higher) than the CTL simulation during summer (winter), especially for the drought years 2002-2003, leading to a good agreement between OGN and observations for 2<sup>nd</sup> and 3<sup>rd</sup> layer soil temperature (Figure 4b, c).”, or by “However, for deep layers (10-100cm), the OGN soil temperature has a good agreement with the observations, which does not occur in the CTL simulation.”

*Revised the sentence to read as “However, for deep layers (10-100cm), soil temperature from the OGN is lower (higher) than the CTL simulation during summer (winter), especially for the drought years 2002-2003, leading to a good agreement between OGN and observations for 2<sup>nd</sup> and 3<sup>rd</sup> layer soil temperature (Figure 4b, c).”*

Lines 227-228: Compared with?

*The original text is not clear and now revised to read “In summer, due to lower saturated thermal conductivity (0.25 W/m K for organic compared to ~6.04 W/m K for mineral) in OGN, the downward transfer of heat from topsoil layer is less and the deep soil temperature in OGN is lower than that in CTL. In winter, with the presence of soil ice, the thermal heat conductivity in OGN (~2.20 W/m K) is lower than that in CTL (6.04 W/m K), it reduces the upward transfer of heat from deep soils to topsoil and therefore results in higher deep-soil temperature in OGN.”*

|

**The incorporation of an organic soil layer in the Noah-MP Land Surface Model and its  
evaluation over a Boreal Aspen Forest**

Liang Chen<sup>1,2</sup>, Yanping Li<sup>1</sup>, Fei Chen<sup>3</sup>, Alan Barr<sup>4</sup>, Michael Barlage<sup>3</sup>, and Bingcheng Wan<sup>3</sup>

<sup>1</sup>Global Institute for Water Security, University of Saskatchewan, Saskatoon, SK, Canada

<sup>2</sup>Key Laboratory of Regional Climate Environment for Temperate East Asia, Institute of  
Atmospheric Physics, Chinese Academy of Sciences, Beijing, China

<sup>3</sup>National Center for Atmospheric Research, Boulder, Colorado

<sup>4</sup>Environment Canada, National Hydrology Research Center, Saskatoon, SK, Canada

*Corresponding author address:*

Yanping Li

Global Institute for Water Security

School of Environment and Sustainability

University of Saskatchewan

Phone: 306-966-2793

E-mail: yanping.li@usask.ca

## Abstract

A thick top layer of organic matter is a dominant feature in boreal forests and can impact land-atmosphere interactions. In this study, the multi-parameterization version of the Noah land-surface model (Noah-MP) was used to investigate the impact of incorporating a forest-floor organic soil layer on the simulated surface energy and water cycle components at the BERMS Old Aspen Flux (OAS) field station in central Saskatchewan, Canada. Compared to a simulation without an organic soil parameterization (CTL), the Noah-MP simulation with an organic soil (OGN) improved Noah-MP simulated soil temperature profiles and soil moisture at 40-100cm, especially the phase and amplitude (Seasonal cycle) of soil temperature below 10 cm. OGN also enhanced the simulation of sensible and latent heat fluxes in spring, especially in wet years, which is mostly related to the timing of spring soil thaw and warming. Simulated top-layer soil moisture is better in OGN than that in CTL. The effects of including an organic soil layer on soil temperature are not uniform throughout the soil depth and are more prominent in summer. For drought years, the OGN simulation substantially modified the partitioning of water between direct soil evaporation and vegetation transpiration. For wet years, the OGN simulated latent heat fluxes are similar to CTL except for spring season where OGN produced less evaporation, which was closer to observations. Including organic soil produced more sub-surface runoff and resulted in much higher runoff throughout the freezing periods in wet years.

Deleted: in summer but worse in winter

Deleted: season

**Keywords** Organic soil, Noah-MP, surface energy and water budgets, BERMS

1 **1. Introduction**

2 Land surface processes play an important role in the climate system by controlling land-  
3 atmosphere exchanges of momentum, energy and mass (water, carbon dioxide, and aerosols).  
4 Therefore, it is critical to correctly represent these processes in land surface models (LSMs) that  
5 are used in weather prediction and climate models (e.g., Dickinson et al. 1986; Sellers et al. 1996;  
6 Chen and Dudhia 2001; Dai et al. 2003; Oleson et al. 2008, Niu et al. 2011). Niu et al. (2011)  
7 and Yang et al. (2011) developed the Noah LSM with multi-parameterization options (Noah-MP)  
8 and evaluated its simulated seasonal and annual cycles of snow, hydrology, and vegetation in  
9 different regions. Noah-MP has been implemented in the community Weather Research and  
10 Forecasting (WRF) model (Burlage et al. 2015), which is widely used as a numerical weather  
11 prediction and regional climate model for dynamical downscaling in many regions world-wide  
12 (Chotamonsak et al., 2012). The performance of Noah-MP was previously evaluated using in-  
13 situ and satellite data (Niu et al. 2011, Yang et al. 2011, Cai et al. 2014, Pilotto et al. 2015, Chen  
14 et al. 2014). Those evaluation results showed significant improvements in modeling runoff, snow,  
15 surface heat fluxes, soil moisture, and land skin temperature compared to the Noah LSM (Chen  
16 et al. 1996, Ek et al. 2003). Recently, Chen et al. (2014) compared Noah-MP to Noah and four  
17 other LSMs regarding the simulation of snow and surface heat fluxes at a forested site in the  
18 Colorado Headwaters region, and found a generally good performance of Noah-MP. However, it  
19 is challenging to parameterize the cascading effects of snow albedo and below-canopy  
20 turbulence and radiation transfer in forested regions as pointed out by Clark et al. (2015) and  
21 Zheng et al. (2015).

22 The Canadian boreal region contains one third of the world's boreal forest, approximately  
23 6 million km<sup>2</sup> (Bryant et al. 1997). The boreal forests have complex interactions with the

24 atmosphere and have significant impacts on regional and global climate (Bonan, 1991; Bonan et  
25 al., 1992; Thomas and Rowntree, 1992; Viterbo and Betts, 1999; Ciais et al., 1995). Several field  
26 experiments were conducted to better understand and model these interactions, including  
27 BOREAS (Boreal Ecosystem Atmosphere Study) and BERMS (Boreal Ecosystem Research and  
28 Monitoring Sites). Numerous studies have evaluated LSMs using the BOREAS and BERMS  
29 data (Bonan et al. 1997). Levine and Knox (1997) developed a frozen soil temperature (FroST)  
30 model to simulate soil moisture and heat flux and used BOREAS northern and southern study  
31 areas to calibrate the model. They found that soil temperature was underestimated and large  
32 model biases existed when snow was present. Bonan et al. (1997) examined NCAR LSM1 with  
33 flux-tower measurements from the BOREAS, and found that the model reasonably simulated the  
34 diurnal cycle of the fluxes. Bartlett et al. (2002) used the BOREAS Old Jack Pine (OJP) site to  
35 assess two different versions of CLASS, the Canadian Land Scheme (2.7 and 3.0) and found that  
36 both versions underestimated the snow depth and soil temperature values, especially the version  
37 CLASS 2.7.

38 Boreal forest soils often have a relatively thick upper organic horizon. The thickness of  
39 the organic horizon directly affects the soil thermal regime and soil hydrological processes.  
40 Compared with mineral soil, the thermal and hydraulic properties of the organic soil are  
41 significantly different. Dingman (1994) found that the mineral soil porosity ranges from 0.4 to  
42 0.6, while the porosity of organic soil is seldom less than 0.8 (Radforth et al., 1977). The  
43 hydraulic conductivity of organic soil horizons can be very high due to the high porosity (Boelter,  
44 1968). Less suction is observed for given volumetric water content in organic soils than in  
45 mineral soils except when it reaches saturation. The thermal properties of the soil are also  
46 affected by the underground hydrology. Organic soil horizons also have relatively low thermal

Deleted: indirectly affects  
Deleted:

49 conductivity, relatively high heat capacity and a relatively high fraction of plant-available water.  
50 Prior studies illustrated the importance of parameterizing organic soil horizons in LSMs for  
51 simulating soil temperature and moisture (e.g., Letts et al. 2000, Beringer et al. 2001, Molders  
52 and Romanovsky 2006, Nicolsky et al. 2007, Lawrence and Slater 2008).

53 The current Noah-MP model does not include a parameterization for organic soil  
54 horizons. It is thus critical to evaluate the effects of incorporating organic matter on surface  
55 energy and water budgets in order to enhance the global applicability of the WRF-Noah-MP  
56 coupled modeling system. Here we conduct a detailed examination of the performance of the  
57 Noah-MP model in a Canadian boreal forest site. The main objective of this research is to  
58 enhance the modeling of vertical heterogeneity (such as organic matter) in soil structures and to  
59 understand its impacts on the simulated seasonal and annual cycle of soil moisture and surface  
60 heat fluxes. We recognize that Noah-MP has weaknesses in existing sub-process  
61 parameterizations, while the goal of this study is to explore the impact of incorporating organic  
62 soil on surface energy and water budgets, rather than comprehensively addressing errors in  
63 existing Noah-MP parameterization schemes. In this paper, we present the BERMS observation  
64 site in central Saskatchewan (Section 2), and our methodology for conducting 12-year Noah-MP  
65 simulations with and without organic soil layer for that boreal forest site (Section 3). Section 4  
66 discusses the simulations of the diurnal and annual cycles of the surface energy and hydrological  
67 components, in dry and wet periods. Summary and conclusions are given in Section 5.

68

## 69 **2. BERMS site descriptions**

70 The Old Aspen Site (OAS, 53.7°N, 106.2°W, altitude 601 m) is located in mature  
71 deciduous broadleaf forest at the southern edge of the Canadian boreal forest in Prince Albert

72 National Park, Saskatchewan, Canada (Figure 1). The forest canopy consists of a 22-m trembling  
73 aspen overstory (*Populus tremuloides*) with ~10% balsam poplar (*Populus balsamifera*.) and a 2-  
74 m hazelnut understory (*Corylus cornuta*) with sparse alder (*Alnus crispa*). The fully-leafed  
75 values of the leaf area index varied among years from 2.0 to 2.9 for the aspen overstory and 1.5  
76 to 2.8 for the hazelnut understory (Barr et al. 2004). The forest was regenerated after a natural  
77 fire in 1919, and in 1998 it had a stand density of ~830 stems ha<sup>-1</sup>. The soil is an Orthic Gray  
78 Luvisol (Canadian Soil Classification System) with an 8-10 cm deep forest-floor (LFH) organic  
79 horizon overlying a loam Ae horizon (0-21 cm), a sandy clay loam Bt horizon (21-69 cm), and a  
80 sandy clay loam Ck horizon (69+ cm). 30% of the fine roots are in the LFH horizon and 60% are  
81 in the upper 20 cm of mineral soil. The water table lies from 1 to 5 m below the ground surface,  
82 varying spatially in the hummocky terrain and varying in time in response to variations in  
83 precipitation. A small depression near the tower had ponded water at the surface during the wet  
84 period from 2005 to 2010. Mean annual air temperature and precipitation at the nearest long-  
85 term weather station are 0.4 °C and 467 mm, respectively (Waskesiu Lake, 53°55'N, 106°04'W,  
86 altitude 532 m, 1971-2000 climatic normal).

87 Air temperature and humidity were measured at 36-m above ground level using a Vaisala  
88 model HMP35cf or HMP45cf temperature/humidity sensor (Vaisala Oyj, Helsinki, Finland) in a  
89 12-plate Gill radiation shield (R.M. Young model 41002-2, Traverse City, MI, USA). Windspeed  
90 was measured using a propeller anemometer (R.M. Young model 01503-, Traverse City, MI,  
91 USA) located at 38-m above ground level. Atmospheric pressure was measured using a  
92 barometer (Setra model SBP270, distributed by Campbell Scientific Inc., Logan, UT, USA). Soil  
93 temperature was measured using thermocouples in two profiles at depths of 2, 5, 10, 20, 50 and  
94 100 cm. The two upper measurements were in the forest-floor LFH. Soil volumetric water

Deleted:

Deleted:

97 content was measured using TDR probes (Moisture Point Type B, Gabel Corp., Victoria, Canada)  
98 with measurements at depths of 0-15, 15-30, 30-60, 60-90 and 90-120 cm. Three of the eight  
99 probes that were the most free of data gaps were used in this analysis. The TDR probes were  
100 located in a low-lying area of the site that was partially flooded after 2004, resulting in high  
101 Volumetric Water Content (VWC) values that may not be characteristic of the flux footprint.  
102 VWC is also measured at 2.5- and 7.5-cm depth in the forest-floor LFH layer using two profiles  
103 of soil moisture reflect meters (model CS615, Campbell Scientific Inc., Logan, UT, USA),  
104 inserted horizontally at a location that did not flood.

105 Eddy-covariance measurements of the sensible and latent heat flux densities were made  
106 at 39 m above the ground from a twin scaffold tower. Details of the eddy-covariance systems are  
107 given in Barr et al. (2006). Data gaps were filled using a standard procedure (Amiro et al. 2006).

108 The net radiation flux density,  $R_n$ , was calculated from component measurements of  
109 incoming and outgoing shortwave and longwave radiation, made using paired Kipp and Zonen  
110 (Delft, The Netherlands) model CM11 pyranometers and paired Eppley Laboratory (Newport, RI,  
111 USA) model PIR pyrgeometers. The upward-facing radiometers were mounted atop the scaffold  
112 flux tower in ventilated housings to minimize dew and frost on the sensor domes. The net  
113 radiometer and the downward-facing radiometers were mounted on a horizontal boom that  
114 extended 4 m to the south of the flux tower, ~ 10 m above the forest canopy. Details of the minor  
115 terms in the surface energy balance; including soil heat flux and biomass heat storage flux are  
116 given in Barr et al. (2006). During the warm season when all components of the surface energy  
117 balance were resolved, the sum of the eddy-covariance sensible and latent heat fluxes  
118 underestimated the surface available energy (net radiation minus surface storage) by ~15% (Barr  
119 et al. 2006).

120

### 121 **3. Methodology**

#### 122 *3.1 The Noah-MP Land-Surface Model*

123 Noah-MP is a new-generation of LSM, which was developed to improve the performance  
124 of the Noah LSM (Chen et al. 1996; Chen and Dudhia 2001). It is coupled to the WRF  
125 community weather and regional climate model (Barlage et al. 2015), and also available as a  
126 stand-alone 1-D model (Noah-MP v1.1). Noah-MP simulates several biophysical and  
127 hydrological processes that control fluxes between the surface and the atmosphere. These  
128 processes include surface energy exchange, radiation interactions with the vegetation canopy and  
129 the soil, hydrological processes within the canopy and the soil, a multi-layer snowpack with  
130 freeze-thaw, groundwater dynamics, stomatal conductance, and photosynthesis and ecosystem  
131 respiration. The major components include a 1-layer canopy, 3-layer snow, and 4-layer soil.  
132 Noah-MP provides a multi-parameterization framework that allows using the model with  
133 different combinations of alternative process schemes for individual processes (Niu et al., 2011).  
134 Alternative sub-modules for 12 physical processes can provide more than 5000 different  
135 combinations. Soil water fluxes are calculated by the Richards equation using a Campbell/Clapp-  
136 Hornberger parameterization of the hydraulic functions (Clapp and Hornberger, 1978).

137 We use an off-line stand-alone 1-D mode (Noah-MP) with four soil layers: 0-10cm, 10-  
138 40cm, 40-100cm, and 100-200 cm. The selected Noah-MP physics options used in this study are  
139 similar to Barlage et al. (2015), Gao et al. (2015) and Chen et al. (2014) and are list in Table 1. In  
140 the default configuration of Noah-MP, the entire vertical soil profile was treated as one mineral  
141 ground texture only, and no organic soil matter is included.

142 The OAS research site has an organic LFH (forest-floor) soil horizon, 8~10 cm deep.  
 143 This study evaluates the impact of adding an organic soil horizon in the Noah-MP model using a  
 144 similar approach to Lawrence and Slater (2008), which parameterizes soil thermal and  
 145 hydrologic properties in terms of carbon density in each soil layer. Soil carbon or organic  
 146 fraction for each layer is determined as

$$147 \quad f_{sc,i} = \frac{\rho_{sc,i}}{\rho_{sc,max}} \quad (1)$$

148 where  $f_{sc,i}$  is the carbon fraction of the each layer,  $\rho_{sc,i}$  is the soil carbon density, and  $\rho_{sc,max}$  is

149 the maximum possible value (peat density of 130 kg m<sup>-3</sup>, Farouki 1981). In this study, we  
 150 assume that the top-soil layer is made up of 100% organic matter, consistent with the 8-10 cm

151 LFH horizon at OAS, with the carbon fraction equals to 1. The soil properties for this layer are  
 152 calculated based on the parameters of organic soil. The second layer of the soil is considered as  
 153 transition layer and made up of 30% organic matter with the carbon fraction equals to 0.3. The  
 154 soil properties for this layer are specified as a weighted combination of organic and mineral soil  
 155 properties;

$$156 \quad P = (1 - f_{sc,i})P_m + f_{sc,i}P_o \quad (2)$$

157 where  $P_m$  is the value for mineral soil,  $P_o$  is the value for organic soil, and  $P$  is the weighted  
 158 average. The remaining soil layers were assumed to be 100% mineral soil, with the carbon

159 fraction equals to 0, the soil properties for this layer are calculated based on the parameters of  
 160 mineral soil. To investigate impacts of uncertainties of those parameters on simulations, we  
 161 conducted sensitive tests for key parameters such as saturated hydraulic conductivity, porosity,  
 162 suction, and Clapp and Hornberger parameter. Those parameters were perturbed within a 5-20%  
 163 range (except for hydraulic conductivity that is changed over 4 times below and above the

Deleted: The soil properties for each layer are specified as a weighted combination of organic and mineral soil prop[... [1]

Deleted: of the soil

Deleted: ;

Deleted: The second layer of the soil is made up of 30% organic matter as a transition layer, with the carbon fraction equals to 0.3.

Deleted: t

Deleted: .

Field Code Changed

Deleted: quantity

Deleted:

Deleted: that made up of

177 default value) following the work of Letts et al. (2000). Results showed that the simulated top  
178 layer soil moisture is very sensitive to porosity, saturated hydraulic conductivity, saturated matric  
179 potential and Clapp and Hornberger parameter, while other layers are not too sensitive to those  
180 parameters. For porosity, as the value increased, the top soil moisture increased significantly.  
181 The saturated hydraulic conductivity mainly influences the unfrozen period. As the value  
182 increased, the top soil moisture decreased. Saturated matric potential and the Clapp and  
183 Hornberger parameter only influence the frozen period. For saturated matric potential, the top  
184 soil moisture decreased when the parameter value increased. While for Clapp and Hornberger  
185 parameter, the top soil moisture increased when the parameter value increased. Based on the site  
186 measurement, the soil bulk density of the top layer is about 160 kg m<sup>-3</sup>. As described in Letts et  
187 al. (2000), this organic soil can be defined as hemic peat, a medium humified organic soil. Table  
188 2 gives the recommended parameters for hemic peat, with 0.88, 2.0, 0.0102, and 6.1 for porosity,  
189 saturated hydraulic conductivity, saturated matric potential and Clapp and Hornberger parameter,  
190 respectively (Letts et al., 2000). From the sensitivity test mentioned above, it seems that the  
191 recommended values from Letts et al. (2000) produced soil moisture and soil temperature close  
192 to observations.

Deleted: not

### 194 3.2 Forcing data

195 The 30-min meteorological observations, including air temperature, specific humidity,  
196 wind speed, pressure, precipitation, downward solar, and longwave radiation, at 36-m height  
197 from OAS were used as atmospheric forcing data to drive Noah-MP in an off-line 1-D mode.  
198 Figure 2 shows the annual mean temperature (1.5 °C) and total precipitation (406 mm) at this site  
199 during the study period (1998-2009). The most significant climatic features during the study

Deleted: these parameters perturbations, and the simulated soil moisture and temperature results are not sensitive to the changes in porosity, saturated suction, and hydraulic conductivity. This implies that the model results are not as sensitive to specific soil parameter uncertainty as they are to differences in physical properties between CTL and OGN. Therefore, we decided to use literatures (Lawrence and Slater, 2008, Letts et al., 2000) recommended values instead, which produced soil moisture and soil temperature close to observations (see Table 2).

211 period are a prolonged drought that began in July 2001 and extended throughout 2003, and an  
212 extended wet period from 2004-2007.

213

### 214 3.3 Evaluation of model performance

215 Outputs from the Noah-MP simulations were evaluated against observations, using the  
216 Root Mean Squared Error (RMSE), square of the correlation coefficient ( $R^2$ ), and Index of  
217 Agreement (IOA) (Zhang et al. 2013). The IOA is calculated as

$$218 \quad IOA = 1 - \frac{\sum_{i=1}^N (M_i - O_i)^2}{\sum_{i=1}^N (|O_i - \bar{O}| + |M_i - \bar{O}|)^2} \quad (3)$$

219 Where  $M_i$  and  $O_i$  are simulated and observed values of the same variable, respectively, and  $\bar{O}$   
220 is the mean of the observed values. *IOA* ranges from 0 (no agreement) to 1 (perfect match).

221

## 222 4. Results and Discussions

### 223 4.1 Noah-MP model Spin-up

224 The LSM spin-up is broadly defined as an adjustment processes as the model approaches  
225 its equilibrium following the initial anomalies in soil moisture content or after some abnormal  
226 environmental forcing (Yang et al., 1995). Without spin-up, the model results may exhibit drift  
227 as model states try to approach their equilibrium values. To initialize LSMs properly, the spin-up  
228 time required for LSMs to reach the equilibrium stage needs to be examined first (Chen and  
229 Mitchell 1999, Cosgrove et al. 2003). In this study, model runs for the year 1998 were performed  
230 repeatedly until all the soil-state variables reached the equilibrium state, defined as when the  
231 difference between two consecutive one-year simulations becomes less than 0.1% for the annual

Deleted: can be unstable and

233 means (Cai et al., 2014; Yang et al., 1995). Yang et al. (1995) discussed the spin-up processes by  
234 comparing results from 22 LSMs for grass and forest sites, and showed a wide range of spin-up  
235 timescales (from 1 year to 20 years), depending on the model, state variable and vegetation type.  
236 Cosgrove et al. (2003) used four NLDAS-1 LSMs to discuss the spin-up time at six sub-regions  
237 covering North America, and showed that all models reached equilibrium between one to three  
238 years for all six sub-regions. In this study, we found that it requires 9 years for deep-soil  
239 moisture (100-200 cm layer) in Noah-MP to reach its equilibrium, 8 years for latent heat flux and  
240 evapotranspiration, but only 3 years for the surface soil moisture (Figure 3). Cosgrove et al.  
241 (2003) and Chen et al. (1999) indicated that it takes long time to reach equilibrium especially in  
242 the deep soil layers and sparse vegetation because the evaporation was limited by slow water  
243 diffusion time scales between the surface and deep soil layers. When using the groundwater  
244 component of Noah-MP, it might take at least 250 years to spin-up the water table depth in arid  
245 regions (Niu et al., 2007). Cai et al. (2014) found that water table depth requires less than 10  
246 years to spin-up in a wet region, but more than 72 years for a dry region. For this boreal forest  
247 site where the water table depth is shallower (less than 2.5 m), it takes ~7 years for water table  
248 depth to reach equilibrium. However, the freezing/thawing is a relatively slow process, so we set  
249 10 years for the spin-up time for all the experiments discussed here.

Deleted: selected

Deleted: a

250

#### 251 *4.2 Seasonal cycle of soil temperature and moisture*

252 We defined the simulation without incorporating organic soil as the “control experiment”  
253 (CTL); the simulation with the organic soil incorporated as the “organic layer experiment”  
254 (OGN). We first evaluated the CTL and OGN simulated soil temperature and moisture at the  
255 OAS site in relation to observations for the period of 1998-2009.

Deleted: simulated

259 As shown in Figure 4, the effects of including a 10-cm organic top soil layer, on simulated  
 260 soil temperature are not uniform both throughout the soil depth and during the year. Figure 4a  
 261 shows the CTL and OGN simulations produced nearly identical top-layer temperature which are  
 262 in agreement with the observations except for a low bias in the winter period, especially during  
 263 drought years 2002-2003. However, for deep layers (10-100cm), soil temperature from the OGN  
 264 is lower (higher) than the CTL simulation during summer (winter), especially for the drought  
 265 years 2002-2003, leading to a good agreement between OGN and observations for 2<sup>nd</sup> and 3<sup>rd</sup>  
 266 layer soil temperature (Figure 4b, c). Lawrence and Slater (2008) indicated that strong cooling in  
 267 summer is due to the modulation of early and mid-summer soil heat flux, while higher soil  
 268 temperature in fall and winter is due to less efficient cooling of organic soils. The soil thawing  
 269 period in spring is significantly affected by the OGN parameterization since the thermal  
 270 conductivity of the organic horizon is much lower than that of the mineral soil ( $\sim 0.4 \text{ W m}^{-1} \text{ K}^{-1}$   
 271 compared to  $\sim 2.0 \text{ W m}^{-1} \text{ K}^{-1}$ ), which delays the warming of the deep soil layers after snowmelt.  
 272 In winter, the organic soil layer insulates the soil and results in relatively higher wintertime soil  
 273 temperatures for OGN compared with CTL. The difference is most pronounced in drought years  
 274 (2002 and 2003) (Figure 4). In summer, due to lower saturated thermal conductivity (0.25 W/m  
 275 K for organic compared to  $\sim 6.04 \text{ W/m K}$  for mineral) in OGN, the downward transfer of heat from  
 276 topsoil layer is less and the deep soil temperature in OGN is lower than that in CTL.  
 277 In winter, with the presence of soil ice, the thermal heat conductivity in OGN ( $\sim 2.20 \text{ W/m K}$ ) is  
 278 lower than that in CTL ( $6.04 \text{ W/m K}$ ), it reduces the upward transfer of heat from deep soils to  
 279 topsoil and therefore results in higher deep-soil temperature in OGN. These results are consistent  
 280 with studies that showed a simulated increase in winter soil temperature of up to  $5 \text{ }^\circ\text{C}$  in boreal  
 281 regions when including an organic layer (Koven et al., 2009; Rinke et al., 2008; Lawrence and  
 282 Slater, 2008) in LSMs.

- Deleted: n
- Deleted: at the top (0-10cm)
- Deleted: and
- Deleted: simulated much
- Deleted: soil temperatures
- Deleted: when the thinner snowpack provides less insulation, leading to higher evaporation, which reduces soil moisture
- Deleted: With an organic soil horizon
- Formatted: Not Highlight
- Deleted: the top soil layer is warmer than the layers beneath it, thus heat is gained by the deep soil. While the heat gained is lower for OGN compared with CTL due to the low thermal heat conductivity of uppermost organic soil layers ( $\sim 0.25 \text{ W/m K}$  compared to  $\sim 6.04 \text{ W/m K}$ ).
- Deleted: OGN produces lower (higher) liquid soil water content during winter (summer) in the topsoil layer (Figure 5)
- Formatted: Not Highlight
- Formatted: Not Highlight
- Formatted: Indent: First line: 0 ch
- Formatted: Not Highlight
- Deleted: the air temperature is colder than the soil temperature and heat is transferred from the soil column to the air. Lower (Although the higher) soil moisture reduces (increases) thermal heat conductivity of uppermost organic soil is becomes slightly higher because of the higher thermal heat conductivity of ice relative to liquid water ( $\sim 2.20 \text{ W/m K}$  compared to  $\sim 0.57 \text{ W/m K}$ ). However, the value is still much lower than the mineral soil value of  $6.04 \text{ W/m K}$ , and. aAgain the insulating properties of organic soil restrict the cooling of the soil. Therefore, it rand results in higher (lower) winter (summer) soil temperature in OGN as compared to CTL.
- Formatted: Not Highlight

310 For the top soil layer, the OGN parameterization increases the liquid soil water content in  
311 summer as water fills the larger pore space of organic soil, ~~though~~, the liquid soil water content in  
312 winter ~~didn't change much~~, due to the contrasting water retention characteristics of organic and  
313 mineral soil (Koven et al., 2009; Rinke et al., 2008; Lawrence and Slater, 2008). Higher porosity  
314 in OGN leads to an increase in total soil water content, while lower the topsoil temperature,  
315 (Figure 4a) in OGN ~~enhances~~, the ice content. Note that the observed soil water content during  
316 wet years may be higher than the site truth because the sensors were located in a low spot that is  
317 prone to flooding. This site got flooded in 2004 and the ground water has not dried since then, so  
318 that the soil was oversaturated during the period of 2004-2008. In the second soil layer, the  
319 observed soil water content was incorrect after the site got flooded (2004-2008). With more  
320 precipitation ~~during the wet period~~, the real soil water content should have a relatively high value.  
321 Since the OGN increases the soil water content, it should be closer to the true observation. From  
322 ~~Figure 5~~, it can be seen that the OGN improved the liquid water simulation in non-frozen periods.  
323 The soil moisture data are not reliable when the soil is frozen and are therefore not very useful  
324 during the winter. In late spring when snow starts melting, both CTL and OGN simulate the  
325 same topsoil temperature (Figure 4). It is clear that the soil liquid water content is mainly  
326 controlled by precipitation, soil hydraulic conductivity and runoff. The high porosity of organic  
327 soil in the topsoil layer helps to retain more snowmelt water and hence increases the topsoil layer  
328 liquid water content. For the deep soil layers, the soil liquid water content is highly influenced by  
329 the soil temperature. Liquid soil water content increases during soil ice thawing period. The  
330 higher deep soil layer liquid water content in OGN is mainly because the soil hydraulic  
331 conductivity is higher for organic soil than mineral soil, so liquid water in the first-layer can be  
332 transported downward quickly into the deeper layers. Although the organic soil layer is only

Deleted: but

Deleted: decreases

Deleted: s

Deleted: with

Deleted: d

Deleted: for

Deleted: is

Deleted: f

341 added to the first two layers in this study, it still can affect the deep layer due to the infiltration  
342 characteristics of the topsoil.

Deleted: top

343 The water retention characteristics of the organic soil horizon favor both higher water  
344 retention and reduced evaporation. The thermal conductivity is lower compared with that of the  
345 mineral soil, which then prevents the deeper soil to warm up rapidly after snowmelt season. The  
346 lower thermal conductivity of the top organic soil affects the annual cycle of the ground heat flux.  
347 In summer, the top layer is warmer than the deep layers, the ground heat flux then transfers heat  
348 downward. Because air temperature is lower than land surface temperature so heat is transferred  
349 upward from soil to the land surface, the low thermal conductivity of the organic soil can prevent  
350 the soil to cool. On the other hand, the snowfall in winter may form a snow layer that will  
351 insulate the soil and make the simulations less sensitive to thermal conductivity. This may be the  
352 reason why the OGN simulated winter soil temperature is higher compared to CTL simulations.

Deleted: er

353 With the organic soil layer on the top, the reduction of surface layer saturation levels in winter  
354 time (Figure 5) reduces the heat loss through evaporation. The winter soil temperature then  
355 becomes significantly higher compared with CTL experiment. On the contrary, the higher soil  
356 water content in the topsoil layer during summer time (Figure 5) increases the heat loss through  
357 evaporation, the summer soil temperature then becomes significantly lower compared with CTL  
358 experiment.

Deleted: increased

Deleted: in winter

Deleted: the lower liquid soil water content in the topsoil layer during

Deleted: ;

Deleted: t

Deleted: ,

Deleted: Wwhile

Deleted:

Deleted: ;

359  
360 *4.3 Seasonal cycles of sensible and latent heat flux*

361 Simulated differences in top-layer soil temperature and liquid soil water content lead to  
362 the differences in simulated surface energy fluxes. Figure 6 show that the CTL run captures the  
363 observed monthly mean daytime sensible heat and latent heat flux reasonably well. However, SH

376 is underestimated in spring and overestimated in summer. Accordingly, LH is overestimated in  
377 spring and underestimated in summer during most of the time period except for drought years  
378 2002-2003 where LH is slightly overestimated. Generally, the OGN simulations show similar  
379 characteristics to the CTL, with improved correlation coefficients between observations and  
380 simulations: increasing from 0.88 (CTL) to 0.92 (OGN) for SH and from 0.94 (CTL) to 0.96  
381 (OGN) for LH (Figure 7). Overall, both CTL and OGN perform well in winter when snow is  
382 present and fluxes are small. During the spring snow-melting season, the OGN results are much  
383 better than the CTL (Figures 6 and 7).

384 The OGN simulations also improved the underestimation of SH in spring in CTL, but it  
385 still overestimates summer SH. The reason for high bias in summer SH will be further discussed  
386 in Section 4.4. SH and especially LH show improvement in OGN compared to CTL, which is  
387 related to timing of soil thaw and warming in spring. CTL thaws the soil too early causing a  
388 premature rise in LH in spring (April-May) and an associated underestimation of spring SH. The  
389 spring (April-May) fluxes are much improved in the OGN parameterization. However, both  
390 OGN and CTL retain a serious positive bias in SH from June-September, especially for wet years.  
391 The reduction of surface layer saturation levels in OGN led to lower soil evaporation and  
392 associated reductions in the total latent heat flux, and the reduction of LH is accompanied by a  
393 rise in SH (Figure 6).

394

#### 395 4.4 Impact of organic soil on diurnal cycle of surface energy and hydrology

396 The quality of nighttime flux-tower data is questionable (Chen et al. 2015), especially for  
397 OAS located in a boreal forest. Therefore, we focused our analysis on daytime observation data.  
398 In general, the OGN parameterization improved the simulation of daily daytime LH in terms of

Deleted: 1  
Deleted: 876  
Deleted: 56  
Deleted: better  
Deleted: ith  
Deleted: cover, and the differences between CTL and OGN is small

Deleted: at

407 both RMSE and IOA, and increased IOA for SH (Table 3). Nevertheless, compared with CTL,  
408 OGN increased the bias in SH slightly by ~3% (Table 3).

Deleted: 6

409 For the 12-year simulation period, the study site experienced a prolonged drought,  
410 beginning in July 2001 and extended throughout 2002 and 2003. We choose year 2002 and 2003  
411 to represent typical drought years, and year 2005 and 2006 to represent typical wet years (Figure  
412 2), to examine the effect of the organic soil under different climate conditions. For drought years

413 2002-2003, OGN increased daytime SH especially in spring, and slightly decreased SH at  
414 nighttime (Figure 8a, b, c, and d). LH is well simulated in both OGN and CTL (Figure 8e, f, g,  
415 and h), with slightly increased daytime LH in OGN. OGN overestimates daytime SH compared  
416 with observations, while CTL underestimates daytime SH for spring (Figure 8a). Both OGN and  
417 CTL overestimates SH for summer, autumn and winter (Figure 8b, c, d).

Deleted: (  
Deleted: )  
Deleted: by

Deleted: OGN  
Deleted: reducing  
Deleted: slightly  
Deleted: and b  
Deleted: slightly

418 For wet years (Figure 9), OGN produces in general higher daytime SH than CTL. For  
419 spring, OGN simulated SH agrees with the observation better than CTL, but it is similar to or  
420 slightly worse than CTL for other seasons. Simulated LH for both OGN and CTL agree with  
421 observations well, with an improvement by OGN in spring, because the snowmelt process  
422 dominates during spring months. For other seasons, the OGN results are close to CTL.

Deleted: OGN has a major impact on the daily cycle of soil temperature. Consistent with discussions in Section 4.2, the soil temperature below 10 cm simulated by OGN is lower in summer and higher in winter than that of the CTL simulation, and the OGN simulation has less bias than the CTL simulation (Figure 4). In OGN simulation, the water moves faster into deep layers than in CTL simulation, leading to more infiltrated water in the deep soil and hence higher base flow. Consequently, the total runoff is increased. Due to the high soil porosity of the organic soil, OGN simulation shows higher soil-ice fraction at the top soil layer during the freezing periods. The higher water capacity and higher soil-ice fraction of the organic soil then reduce liquid water content/soil moisture, these further lead to less evaporation (i.e., latent heat flux) during freezing periods (Spring), and a compensating increase of the sensible heat flux.

423 It is clear from Figures. 4, 8 and 9 that in both CTL and OGN, summer sensible heat  
424 fluxes are overestimated for wet and dry years. We hypothesized that such high bias in summer  
425 sensible heat flux is partly attributed to energy imbalance in observations. We then calculated the  
426 energy balance residual term:  $R_{net}-(SH+LH+G)$  for summer month (June, July, and August). In  
427 wet years,  $G_v$  in CTL, and OGN is close to observed values; modeled latent heat flux is  
428 underestimated by  $\sim 10 \text{ W/m}^2$ ; modeled sensible heat flux is overestimated by  $\sim 30 \text{ W/m}^2$ ; and the  
429 residual term is  $\sim 17 \text{ W/m}^2$ . Hence, it is reasonable to argue that the surface energy imbalance

Deleted: significant  
Deleted: . Note that the OGN simulation also improves latent heat fluxes significantly in drought years  
Deleted: fairly  
Deleted: ,  
Deleted: and  
Deleted: FX  
Deleted: LT

463 (~17 W/m<sup>2</sup>) in observations contributes to a large portion of the ~30 W/m<sup>2</sup> high bias in sensible  
464 heat fluxes. In dry years, the summer energy imbalance (~15 W/m<sup>2</sup>) is nearly equal to the high  
465 bias in sensible heat flux (~15 W/m<sup>2</sup>).

Deleted: part

Deleted: of the

Deleted:

466

#### 467 4.5 Impact of an organic soil horizon on annual cycle of surface energy and hydrology

468 In the previous section, it is clear that the incorporation of the top organic layer helps  
469 improve the simulation of the diurnal cycle of the surface energy and hydrologic components in  
470 spring season. In the following, we focus on a detailed analysis of the annual cycle of the surface  
471 energy and hydrology variables for "dry" (Figure 10) versus "wet" years (Figure 11). Between  
472 June and September as shown in Figure10h, the upper two soil layers were unfrozen. The topsoil  
473 is wetter in OGN for both dry and wet years compared with CTL because organic soil can retain  
474 more water. As discussed in section 4.2, for the deep soil layers, the liquid water content is  
475 influenced by the soil temperature and the movements of the soil liquid water content between  
476 soil layers. Since the soil hydraulic conductivity is higher for OGN than mineral soil, the water  
477 moves faster into deep soil layers than CTL, therefore the OGN simulates higher soil liquid  
478 water content in deep layers. OGN has a major impact on the daily cycle of soil temperature.  
479 Consistent with discussions in Section 4.2, the soil temperature below 10 cm simulated by OGN  
480 is lower in summer and higher in winter than that of the CTL simulation, and the OGN  
481 simulation shows less bias than the CTL simulation (Figure 4). In OGN simulation, the water  
482 moves faster into deep layers than in CTL simulation, leading to more infiltrated water in the  
483 deep soil and hence higher base flow. Consequently, the total runoff is increased. Due to the high  
484 soil porosity of the organic soil, OGN simulation shows higher soil-ice fraction at the top soil  
485 layer during the freezing periods. The higher water capacity and higher soil-ice fraction of the

Deleted: last

490 organic soil then reduce liquid water content/soil moisture, leading to less evaporation (i.e.,  
491 latent heat flux) during spring freezing periods, and a compensating increase of the sensible heat  
492 flux.

493 By adding an organic soil layer, the soil ice content becomes higher due to higher  
494 porosity. For dry years, the impact of the organic soil on surface and sub-surface runoff is not  
495 significant (Figure 10e, f). The increase in the summer latent heat flux and sensible heat flux are  
496 compensated by a decrease in soil heat flux, leading to a significant decrease in summer soil  
497 temperature. In winter, the latent and sensible heat fluxes are not modified by the organic soil,  
498 but increased soil heat flux leads to an increased soil temperature in winter. The most prominent  
499 change by adding organic soil layer is the partition between vegetation transpiration and direct  
500 ground evaporation (Figure 12a and b) where the OGN simulation slightly increased ground  
501 surface evaporation and vegetation transpiration.

502 For wet years (Figure 11), the impact of the organic soil on surface and sub-surface  
503 runoff becomes more significant, especially for sub-surface runoff. The organic soil decreases  
504 the surface runoff during the summer season, and increases the sub-surface runoff during the  
505 freezing periods while decreases the sub-surface runoff during summer season. Because of the  
506 higher surface layer soil ice content, the increase of subsurface flow should be due to the  
507 producing a wetter soil profile by OGN. The sensible heat flux also increases significantly in  
508 spring, with an associated reduction in latent heat flux and soil heat flux. The summer soil  
509 temperature also decreases but to a lesser degree than that in dry years, because the soil heat flux  
510 decreases less compared with dry years. Unlike dry years, there is a significant runoff change in  
511 wet years, and the ground evaporation is also decreased (Figure 12c and d). OGN produces more  
512 soil-ice content and higher soil porosity, and leads to higher soil water content than CTL

**Deleted:** The total soil column liquid water content keeps increasing before the soil temperature reaches above the freezing point (Figure 10, g, 11, g), which is because the deep soil temperature is usually higher than the top soil so ice get melts earlier in deep layer.  
**Formatted:** Highlight

**Deleted:**

**Deleted:** de

**Deleted:** in

**Deleted:** spring snowmelt

**Deleted:** throughout the year

**Deleted:** OGN

**Deleted:** in

**Deleted:** total

526 simulations as the higher ice content severely restricts movement of water out of the soil column.

527 In wet season, by adding an organic topsoil layer, the soil water increases due to the infiltration  
528 of the soil water into the deep soil. This then leads to an increase in the sub-surface runoff. As a  
529 consequence, the volumetric liquid water becomes higher in summer for OGN compared with  
530 CTL simulation.

531

## 532 5. Summary and Conclusions

533 In this study, the Noah-MP LSM was applied at the BERMS Old Aspen site to  
534 investigate the impact of incorporating a realistic organic soil horizon on simulated surface  
535 energy and water cycle components. This site has an about 8-10 cm deep organic forest-floor soil  
536 horizon, typical of boreal deciduous broadleaf forests. When including, for the first time, an  
537 organic-soil parameterization within the Noah-MP model, simulated sensible heat flux and latent  
538 heat flux are improved in spring, especially in wet years, which is mostly related to the timing of  
539 spring soil thaw and warming. However, in summer the model overestimated sensible heat fluxes.  
540 Such high bias in summer sensible heat flux is largely attributed to surface-energy imbalance in  
541 observations, especially in dry years. Due to lower thermal conductivity, the OGN simulated soil  
542 temperature was decreased during summer and slightly increased during winter compared with  
543 the CTL simulation, and the OGN simulated soil temperature (10-100cm) were more consistent  
544 with observations and with previous studies (Lawrence and Slater 2008). Simulated top-layer  
545 soil moisture is better in OGN than in CTL in summer but worse in winter.

546 Also, due to higher porosity of the organic soil, the OGN simulation was able to retain  
547 more soil water content in summer. However, the effects of including an organic soil layer on

Deleted: total column

Deleted: the

Deleted: -

Deleted:

Deleted: . However, in winter, the OGN experiment produced less liquid soil-water content due to the lower temperature and higher porosity. Since most of the soil moisture is stored in soil ice, the liquid water content is reduced

557 soil temperature are not uniform throughout the soil depth and year, and those effects are more  
558 prominent in summer and in deep soils.

559 For drought years, the OGN simulation substantially modified the partition between  
560 direct soil evaporation and vegetation transpiration. When water is limited in drought years, the  
561 OGN simulation ~~slightly increased~~ the direct soil evaporation ~~and~~ produced higher summer total  
562 evapotranspiration. Increased latent heat flux and sensible heat flux in summer in OGN are  
563 compensated by decreased soil heat flux, leading to reduced soil temperature in summer. For wet  
564 years, the OGN simulated latent heat fluxes are similar to CTL except for spring season where  
565 OGN produced less evaporation. In addition, the impact of the organic soil on sub-surface runoff  
566 is substantial with much higher runoff ~~in freezing periods and lower runoff in summer~~ season.

Deleted: significantly reduced

Deleted: but still

Deleted: throughout the

567 This preliminary study explored the effects of incorporating organic soil parameterization  
568 in Noah-MP on the surface energy and water cycles for one flux site in a boreal forest area.  
569 Given the important role of boreal forests in the regional climate system through reducing winter  
570 albedo and also acting as a carbon sink and water source to the atmosphere, further work is  
571 needed to evaluate the Noah-MP with organic-soil parameterization at regional scales. We plan  
572 to evaluate the performance of the offline Noah-MP model and Noah-MP coupled with WRF for  
573 a broad boreal forest region including Alberta and Saskatchewan.

574

575

576

## 577 **Acknowledgments**

578 The author Liang Chen acknowledge the support from the National Basic Research Program  
579 (Grant No. 2012CB956203) and National Natural Science Foundation of China (Grant No.

583 41305062). The authors Liang Chen, Yanping Li, Alan Barr gratefully acknowledge the support  
584 from Global Institute of Water Security at University of Saskatchewan. Fei Chen, Michael  
585 Barlage and Bingcheng Wan appreciate the support from the Water System Program at the  
586 National Center for Atmospheric Research (NCAR), and NOAA MAPP-CTB grant  
587 (NA14OAR4310186). NCAR is sponsored by the National Science Foundation. Any opinions,  
588 findings, conclusions or recommendations expressed in this publication are those of the authors  
589 and do not necessarily reflect the views of the National Science Foundation.  
590

591 **References**

- 592 Amiro BD, AG Barr, TA Black, H Iwashita, N Kljun, JH McCaughey, K Morgenstern, S  
593 Murayama, Z Nestic, AL Orchansky, and N Saigusa. 2006. Carbon, energy and water fluxes  
594 at mature and disturbed forest sites, Saskatchewan, Canada. *Agric. For. Meteorol.*, 136: 237-  
595 251.
- 596 Ball, J. T., I. E. Woodrow, and J. A. Berry (1987), A model predicting stomatal conductance and  
597 its contribution to the control of photosynthesis under different environmental conditions, in  
598 *Process in Photosynthesis Research*, vol. 1, edited by J. Biggins, pp. 221–234, Martinus  
599 Nijhoff, Dordrecht, Netherlands.
- 600 Barlage, M., Tewari, M., Chen, F., Miguez-Macho, G., Yang, Z. L., and Niu, G. Y. (2015), The  
601 effect of groundwater interaction in North American regional climate simulations with  
602 WRF/Noah-MP, *Climatic Change*, 129(3-4), 485-498.
- 603 Bartlett, P.A., J.H. McCaughey, P.M. Lafleur and D.L. Verseghy (2002), A comparison of the  
604 mosaic and aggregated canopy frameworks for representing surface heterogeneity in the  
605 Canadian boreal forest using CLASS: A soil perspective, *Journal of Hydrology*, 266:15-39.
- 606 Barr, A. G., T. A. Black, E. H. Hogg, N. Kljun, K. Morgenstern, and Z. Nestic (2004), Inter-  
607 annual variability in the leaf area index of a boreal aspen-hazelnut forest in relation to net  
608 ecosystem production, *Agricultural and forest meteorology*, 126(3), 237–255.
- 609 Barr, A.G., K. Morgenstern, T. A. Black, J. H. McCaughey, and Z. Nestic (2006), Surface energy  
610 balance closure by the eddy-covariance method above three boreal forest stands and  
611 implications for the measurement of the CO<sub>2</sub> flux, *Agricultural and forest meteorology*, 140,  
612 322-337.

613 Beringer, J., N. J. Tapper, I. McHugh, F. Chapin, A. H. Lynch, M. C. Serreze, and A. Slater  
614 (2001), Impact of arctic treeline on synoptic climate, *Geophysical Research Letters*, 28(22),  
615 4247–4250.

616 Boelter, D. H. (1968), Important physical properties of peat materials. *Proceedings of the 3rd*  
617 *International Peat Congress, Quebec*: 150-156.

618 Bonan, G. B. (1991), Atmosphere-biosphere exchange of carbon dioxide in boreal forests, *J.*  
619 *Geophys. Res.*, 96(D4), 7301–7312, doi: 10.1029/90JD02713.

620 Bonan, G. B., D. Pollard, and S. L. Thompson. 1992. Effects of Boreal Forest Vegetation on  
621 Global Climate. *Nature*, 359: 716-18.

622 Bonan, G. B. (1997), Effects of land use on the climate of the United States, *Climatic Change*, 37,  
623 449–486.

624 Brutsaert, W. A. (1982), *Evaporation Into the Atmosphere*, 299 pp., D. Reidel, Dordrecht,  
625 Netherlands.

626 Bryant, D., D. Nielsen, and L. Tanglely (1997), *The Last Frontier Forests: Ecosystems and*  
627 *Economies on the Edge*. World Resources Institute.

628 Cai, X., Z. L. Yang, C. H. David, G. Y. Niu, and M. Rodell (2014), Hydrological evaluation of  
629 the Noah - MP land surface model for the Mississippi River Basin, *Journal of Geophysical*  
630 *Research: Atmospheres*, 119(1), 23-38.

631 Chen, F., J. Dudhia (2001), Coupling an advanced land surface-hydrology model with the Penn  
632 State-NCAR MM5 modeling system. Part I: Model implementation and sensitivity, *Monthly*  
633 *Weather Review*, 129(4), 569-585.

634 Chen, F., K. Mitchell, J. Schaake, Y. Xue, H. L. Pan, V. Koren, Q. Y. Duan, M. Ek, and A. Betts  
635 (1996), Modeling of land surface evaporation by four schemes and comparison with five

636 observations, *Journal of Geophysical Research: Atmospheres* (1984–2012), 101(D3), 7251–  
637 7268.

638 Chen, F., M. J. Barlage, M. Tewari, R. M. Rasmussen, J. Jin, D. Lettenmaier, B. Livneh, C. Lin,  
639 G. Miguez-Macho, G. Y. Niu, L. Wen, and Z. L. Yang (2014), Modeling seasonal snowpack  
640 evolution in the complex terrain and forested Colorado Headwaters region: A model  
641 intercomparison study, *Journal of Geophysical Research-Atmospheres*, 119, 13795-13819,  
642 DOI: 10.1002/2014JD022167.

643 Chen, F. and K. Mitchell (1999), Using GEWEX/ISLSCP forcing data to simulate global soil  
644 moisture fields and hydrological cycle for 1987-1988, *Journal of the Meteorological Society*  
645 of Japan, 77, 1-16.

646 Chen F., G. Zhang, M. Barlage, Y. Zhang, J. A. Hicke, A. Meddens, G. Zhou, W. J. Massman,  
647 and J. Frank (2015), An Observational and Modeling Study of Impacts of Bark Beetle-  
648 Caused Tree Mortality on Surface Energy and Hydrological Cycles. *J. Hydrometeorol*, 16,  
649 744–761, doi: <http://dx.doi.org/10.1175/JHM-D-14-0059.1>

650 Chotamonsak, C., E. P. Salathe Jr, J. Kreasuwan, and S. Chantara (2012), Evaluation of  
651 precipitation simulations over Thailand using a WRF regional climate model. *Chiang Mai*  
652 *Journal of Science*, 39(4), 623-638.

653 Ciais, P., P. P. Tans, M. Trolier, J. W. C. White, and R. J. Francey (1995), A large northern  
654 hemisphere terrestrial CO<sub>2</sub> sink indicated by the <sup>13</sup>C/<sup>12</sup>C ratio of atmospheric CO<sub>2</sub>,  
655 *SCIENCE-NEW YORK THEN WASHINGTON*, 1098-1098.

656 Clapp, R. B., and G. M. Hornberger (1978), Empirical equations for some soil hydraulic  
657 properties, *Water resources research*, 14(4), 601-604.

Field Code Changed

658 Clark, M. P., et al. (2015), A unified approach for process-based hydrologic modeling: 1.  
659 Modeling concept, *Water Resour. Res.*, 51, 2498–2514, doi:10.1002/2015WR017198

660 Cosgrove, B. A., D. Lohmann, K. E. Mitchell, P. R. Houser, E. F. Wood, J. C. Schaake, A.  
661 Robock, C. Marshall, J. Sheffield, Q. Duan, L. Luo, R. W. Higgins, R. T. Pinker, J. D.  
662 Tarpley, and J. Meng (2003), Real-time and retrospective forcing in the North American  
663 Land Data Assimilation System (NLDAS) project, *J. Geophys. Res.*, 108, 8842, doi:  
664 10.1029/2002JD003118, D22.

665 Dai, Y., X. Zeng, R. E. Dickinson, I. Baker, G. B. Bonan, M. G. Bosilovich, A. S. Denning, P. A.  
666 Dirmeyer, P. R. Houser, G. Niu, K. W. Oleson, C. A. Schlosser, and Z. L. Yang (2003), The  
667 Common Land Model. *Bull. Amer. Meteor. Soc.*, 84, 1013–1023. doi:  
668 <http://dx.doi.org/10.1175/BAMS-84-8-1013>

669 Dickinson, R. E. (1986), Biosphere/atmosphere transfer scheme (bats) for the near com-  
670 munity climate model, Technical report.

671 Dingman, S. L. (1994), *Physical Hydrology*, MacMillan Publishing Company, New York.

672 Ek, M. B., K. E. Mitchell, Y. Lin, E. Rogers, P. Grunmann, V. Koren, G. Gayno, and J. D.  
673 Tarpley (2003), Implementation of Noah land surface model advances in the National  
674 Centers for Environmental Prediction operational mesoscale Eta model, *J. Geophys. Res.*,  
675 108, 8851, doi:10.1029/2002JD003296, D22.

676 Farouki, O. T. (1981), Thermal properties of soils, Report No. Vol. 81, No. 1, CRREL  
677 Monograph

678 Gayler, S., T. Wöhling, M. Grzeschik, J. Ingwersen, H. D. Witzmann, K. Warrach-Sagi, P. Högy,  
679 S. Attinger, T. Streck, and V. Wulfmeyer (2014), Incorporating dynamic root growth

680 enhances the performance of Noah-MP at two contrasting winter wheat field sites, *Water*  
681 *Resour. Res.*, 50, 1337-1356, doi:10.1002/2013WR014634.

682 Jordan, R. (1991), A one-dimensional temperature model for a snow cover, *Spec. Rep.* 91-16,  
683 *Cold Reg. Res. and Eng. Lab.*, U.S. Army Corps of Eng., Hanover, N. H.

684 Koren, V., J. C. Schaake, K. E. Mitchell, Q.-Y. Duan, F. Chen, and J. M. Baker (1999), A  
685 parameterization of snowpack and frozen ground intended for NCEP weather and climate  
686 models, *J. Geophys. Res.*, 104, 19,569-19,585, doi:10.1029/1999JD900232.

687 Koven, C., P. Friedlingstein, P. Ciais, D. Khvorostyanov, G. Krinner, and C. Tarnocai (2009),  
688 On the formation of high-latitude soil carbon stocks: Effects of cryoturbation and insulation  
689 by organic matter in a land surface model, *Geophys. Res. Lett.*, 36, L21501,  
690 doi:10.1029/2009GL040150.

691 Lawrence, D. M., and A. G. Slater (2008), Incorporating organic soil into a global climate model,  
692 *Climate Dynamics*, 30(2-3), 145-160.

693 Letts, M. G., N. T. Roulet, N. T. Comer, M. R. Skarupa, and D. L. Verseghy (2000),  
694 Parametrization of peatland hydraulic properties for the Canadian land surface scheme,  
695 *Atmosphere-Ocean*, 38(1), 141-160.

696 Levine, E. R., and R. G. Knox (1997), Modeling soil temperature and snow dynamics in northern  
697 forests, *J. Geophys. Res.*, 102(D24), 29407-29416, doi:10.1029/97JD01328.

698 Mölders, N., and V. E. Romanovsky (2006), Long-term evaluation of the Hydro-  
699 Thermodynamic Soil-Vegetation Scheme's frozen ground/permafrost component using  
700 observations at Barrow, Alaska, *J. Geophys. Res.*, 111, D04105, doi:10.1029/2005JD005957.

701 Nicolsky, D. J., V. E. Romanovsky, V. A. Alexeev, and D. M. Lawrence (2007), Improved  
702 modeling of permafrost dynamics in a GCM land-surface scheme, *Geophys. Res. Lett.*, 34,  
703 L08501, doi:10.1029/2007GL029525.

704 Niu, G.-Y., and Z.-L. Yang (2006), Effects of frozen soil on snowmelt runoff and soil water  
705 storage at a continental scale, *J. Hydrometeorol.*, 7, 937–952, doi:10.1175/JHM538.1.

706 Niu, G.-Y., Z.-L. Yang, R. E. Dickinson, and L. E. Gulden (2005), A simple TOPMODEL-based  
707 runoff parameterization (SIMTOP) for use in global climate models, *J. Geophys. Res.*, 110,  
708 D21106, doi:10.1029/2005JD006111.

709 Niu, G. Y., Z. L. Yang, K. E. Mitchell, F. Chen, M. B. Ek, M. Barlage, A. Kumar, K. Manning,  
710 D. Niyogi, and E. Rosero (2011), The community Noah land surface model with  
711 multiparameterization options (Noah-MP): 1. Model description and evaluation with local-  
712 scale measurements, *J. Geophys. Res.*, 116, D12109, doi:10.1029/2010JD015139.

713 Oleson, K. W., G. Y. Niu, Z. L. Yang, D. M. Lawrence, P. E. Thornton, P. J. Lawrence, R.  
714 Stöckli, R. E. Dickinson, G. B. Bonan, S. Levis, A. Dai, and T. Qian (2008), Improvements  
715 to the Community Land Model and their impact on the hydrological cycle, *J. Geophys. Res.*,  
716 113, G01021, doi: 10.1029/2007JG000563.

717 Pilotto, I. L., Rodríguez, D. A., Tomasella, J., Sampaio, G., and Chou, S. C. (2015),  
718 Comparisons of the Noah-MP land surface model simulations with measurements of forest  
719 and crop sites in Amazonia. *Meteorology and Atmospheric Physics*, 127(6), 711-723, doi:  
720 10.1007/s00703-015-0399-8.

721 Radforth, N. W. and Brawner, C. O. (1977). Muskeg and the northern environment in Canada. In  
722 Muskeg Research Conference 1973: Edmonton, Alberta. University of Toronto Press.

723 Rinke, A., P. Kuhry, and K. Dethloff (2008), Importance of a soil organic layer for Arctic  
724 climate: A sensitivity study with an Arctic RCM, *Geophys. Res. Lett.*, 35, L13709,  
725 doi:10.1029/2008GL034052.

726 Thomas, G. and Rowntree, P. R. (1992), The Boreal Forests and Climate. *Q.J.R. Meteorol. Soc.*,  
727 118, 469–497. doi: 10.1002/qj.49711850505

728 Verseghy, D. L. (1991), CLASS-A Canadian land surface scheme for GCMS: I. Soil model, *Int.*  
729 *J. Climatol.*, 11, 111–133, doi:10.1002/joc.3370110202.

730 Viterbo, P., and A. K. Betts (1999), Impact on ECMWF forecasts of changes to the albedo of the  
731 boreal forests in the presence of snow, *J. Geophys. Res.*, 104(D22), 27803–27810,  
732 doi:10.1029/1998JD200076.

733 Yang, Z. L., R. E. Dickinson, A. Henderson-Sellers, and A. J. Pitman (1995), Preliminary study  
734 of spin-up processes in land surface models with the first stage data of project for  
735 intercomparison of land surface parameterization schemes phase 1 (a), *Journal of*  
736 *Geophysical Research: Atmospheres*, 100 (D8), 16,553–16,578.

737 Yang, Z.-L., G.-Y. Niu, K. E. Mitchell, F. Chen, M. B. Ek, M. Barlage, L. Longuevergne, K.  
738 Manning, D. Niyogi, M. Tewari, and Y. Xia (2011), The community Noah land surface  
739 model with multiparameterization options (Noah-MP): 2. Evaluation over global river basins,  
740 *J. Geophys. Res.*, 116, D12110, doi:10.1029/2010JD015140.

741 Zhang, G., G. Zhou, F. Chen, M. Barlage, and L. Xue (2014), A trial to improve surface heat  
742 exchange simulation through sensitivity experiments over a desert steppe site, *J.*  
743 *Hydrometeorol.*, 15(2), 664–684, doi:10.1175/jhm-d-13-0113.1.

744 Zheng, D., et al. (2015), Under-canopy turbulence and root water uptake of a Tibetan meadow  
745 ecosystem modeled by Noah-MP, *Water Resour. Res.*, 51, doi:10.1002/2015WR017115  
746

Table 1. Noah-MP Parameterization Options Used in this Study

Parameterizations Description	Options
Dynamic vegetation	4: table LAI, shdfac=maximum
Stomatal resistance	1: BALL-Berry (Ball et al., 1987)
Soil moisture factor for stomatal resistance	1: original Noah (Chen and Dudhia, 2001)
Runoff/soil lower boundary	2: TOPMODEL with equilibrium water table (Niu et al. 2005)
Surface layer drag Coefficient calculation	1: Monin-Obukhov (Brutsaert, 1982)
Supercooled liquid water	1; <del>no iteration (Niu and Yang, 2006)</del>
Soil permeability	1: linear effects, more permeable (Niu and Yang, 2006)
Radiative transfer	3: two-stream applied to vegetated fraction
Ground surface albedo	2: CLASS (Verseghy, 1991)
Precipitation partitioning between snow and rain	1: Jordan (Jordan, 1991)
soil temp lower boundary	2; <del>TBOT at ZBOT (8m) read from a file</del>
snow/soil temperature time	1: semi-implicit

**Deleted:** 2

**Deleted:** Koren's iteration (Koren et al., 1999)

**Formatted:** Font:Times New Roman, 12 pt, Font color: Auto, Pattern: Clear

**Formatted:** Font:Times New Roman, 12 pt, Font color: Auto, Pattern: Clear

**Deleted:** 1

**Formatted:** Font:Times New Roman, 12 pt, Font color: Auto, Pattern: Clear

**Deleted:** zero heat flux

754 Table 2 Soil parameters used in Noah-MP for mineral soil texture classes (SANDY CLAY

755 LOAM) and organic soil (Hemic Peat).

Soil Type	$\lambda_s$ ( $\text{W m}^{-1} \text{K}^{-1}$ )	$\lambda_{\text{sat}}$ ( $\text{W m}^{-1} \text{K}^{-1}$ )	$\lambda_{\text{dry}}$ ( $\text{W m}^{-1} \text{K}^{-1}$ )	$c_s$ ( $\text{J m}^{-3} \text{K}^{-1} \cdot 10^6$ )	$\theta_{\text{sat}}$	$\kappa_{\text{sat}}$ ( $\text{m s}^{-1} \times 10^{-3}$ )	$\psi_{\text{sat}}$ (mm)	$b$
Mineral	6.04	2.24	0.23	2.0	0.421	0.00445	-135	6.77
Organic	0.25	0.55	0.05	2.5	0.88	0.002	-10.3	6.1

756 The soil parameters are  $\lambda_s$  is the thermal conductivity of soil solids,  $\lambda_{\text{sat}}$  is the unfrozen saturated  
 757 thermal conductivity,  $\lambda_{\text{dry}}$  is the dry soil thermal conductivity,  $c_s$  is the soil solid heat capacity,  
 758  $\theta_{\text{sat}}$  is the saturated volumetric water content (porosity),  $\kappa_{\text{sat}}$  is the saturate hydraulic conductivity,  
 759  $\psi_{\text{sat}}$  is the saturated matric potential, and  $b$  is the Clapp and Hornberger parameter.

Deleted: 9

Deleted: 100

Deleted: 2.7

763 **Table 3.** Averaged statistical indices for CTL and OGN simulated SH and LH compared with  
 764 the observations for each year [daytime, 0800-1600 local time (LT)] ( $R^2$ : correlation coefficient  
 765 square; RMSE: root mean square error; IOA: index of agreement).

Year	SH						LH					
	CTL			OGN			CTL			OGN		
	$R^2$	RMSE	IOA									
<b>1998</b>	0.56	80.92	0.83	0.65	81.40	0.85	0.72	51.00	0.91	0.76	47.70	0.93
<b>1999</b>	0.64	64.30	0.88	0.69	68.59	0.88	0.74	44.52	0.92	0.76	43.01	0.93
<b>2000</b>	0.62	71.20	0.87	0.68	74.27	0.88	0.70	47.46	0.90	0.71	46.19	0.91
<b>2001</b>	0.72	63.09	0.90	0.78	66.84	0.91	0.78	40.36	0.93	0.81	36.85	0.95
<b>2002</b>	0.75	69.60	0.91	0.77	71.41	0.92	0.69	37.24	0.91	0.70	39.66	0.91
<b>2003</b>	0.77	56.52	0.93	0.79	56.74	0.94	0.72	36.45	0.91	0.73	42.02	0.90
<b>2004</b>	0.72	61.88	0.91	0.75	64.82	0.92	0.73	39.84	0.92	0.74	40.15	0.92
<b>2005</b>	0.69	60.98	0.90	0.76	60.59	0.92	0.73	43.29	0.92	0.78	39.75	0.94
<b>2006</b>	0.60	67.70	0.86	0.68	70.16	0.88	0.77	49.58	0.93	0.80	45.36	0.94
<b>2007</b>	0.65	65.15	0.89	0.72	65.28	0.90	0.76	46.79	0.93	0.81	42.49	0.95
<b>2008</b>	0.71	63.54	0.91	0.76	68.15	0.91	0.76	44.95	0.93	0.80	40.79	0.95
<b>2009</b>	0.69	66.52	0.90	0.72	69.38	0.90	0.72	43.77	0.91	0.74	43.32	0.92

766

767 **Figure Captions:**

768 **Figure 1.** The location of the study site (Old Aspen Flux Tower)

769 **Figure 2.** Monthly air temperature above canopy and precipitation at BERMS SK-OAS site

770 **Figure 3.** Averaged spin-up time (in years) for individual variables.

771 **Figure 4.** Observed and Noah-MP-simulated monthly soil temperature for BERMS SK-OAS site  
772 at a depth of (a) top 10 cm, (b) 10-40 cm, and (c) 40-100 cm

773 **Figure 5.** Observed and Noah-MP-simulated monthly soil moisture for BERMS SK-OAS site at  
774 a depth of (a) top 10 cm, (b) 10-40 cm, and (c) 40-100 cm

775 **Figure 6.** Observed and the Noah-MP simulated (CTL and OGN) daytime monthly-average  
776 sensible and latent heat flux above canopy. *Error bars represent the average and deviations*  
777  *$[(RN-G) \times B / (1+B)]$  for SH, and  $(RN-G) / (1+B)$  for LH] from observations, and B is the Bowen*  
778 *ratio ( $B=SH/LH$ ).*

779 **Figure 7.** Scatterplots of the daytime monthly-averaged (a) sensible, (b) latent heat fluxes  
780 ( $W m^{-2}$ ) for CTL versus the observation above canopy; the monthly-averaged (c) sensible, (d)  
781 latent heat fluxes ( $W m^{-2}$ ) for OGN versus the observation above canopy. The color represents  
782 each month from January (1) to December (12).

783 **Figure 8.** Comparison of the seasonal averaged diurnal cycle of the sensible and latent heat  
784 fluxes at OAS site for drought years

785 **Figure 9.** Comparison of the seasonal averaged diurnal cycle of the sensible and latent heat  
786 fluxes at OAS site for wet years

787 **Figure 10.** Annual cycle of selected surface energy and hydrologic cycle fields for drought years.

788 Black line is the observation. Note that (a) is the observed precipitation, (b) is sensible heat flux,  
789 (c) is latent heat flux, (d) is ground heat flux, (e) is surface runoff, (f) is underground runoff, (g)

Deleted: Black line is the observation.

791 is ~~volumetric~~ liquid water content ~~for soil layer one~~, (h) is ~~volumetric~~ ice water content ~~for soil~~  
792 ~~layer one~~,

- Deleted: the total column soil
- Deleted: changes
- Deleted: the total column soil
- Deleted: changes

793 **Figure 11.** Annual cycle of selected surface energy and hydrologic cycle fields for wet years.

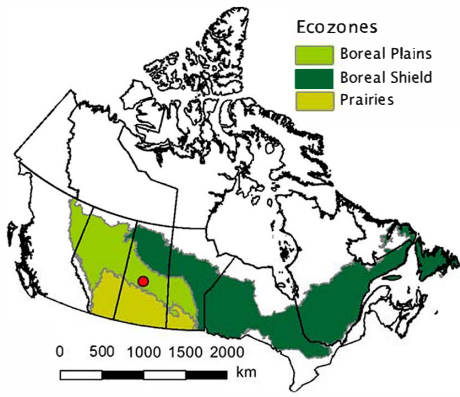
794 Black line is the observation. Note that (a) is the observed precipitation, (b) is sensible heat flux,  
795 (c) is latent heat flux, (d) is ground heat flux, (e) is surface runoff, (f) is underground runoff, (g)

796 is ~~volumetric~~ liquid water content ~~for soil layer one~~, (h) is ~~volumetric~~ ice water content ~~for soil~~  
797 ~~layer one~~,

- Deleted: the total column soil
- Deleted: changes
- Deleted: the total column soil
- Deleted: changes

798 **Figure 12.** Water budgets: blue lines are accumulated surface runoff (mm), blue dots are  
799 accumulated underground runoff (mm), red lines are accumulated evaporation of intercepted  
800 water (mm), red dots are accumulated ground surface evaporation (mm), red dash lines are  
801 accumulated transpiration (mm), green lines are snow water equivalent changes (mm), purple  
802 lines are soil water content changes in the soil column (mm), (a) and (b) are averaged for 2002–  
803 2003, (c) and (d) are averaged for 2005-2006.

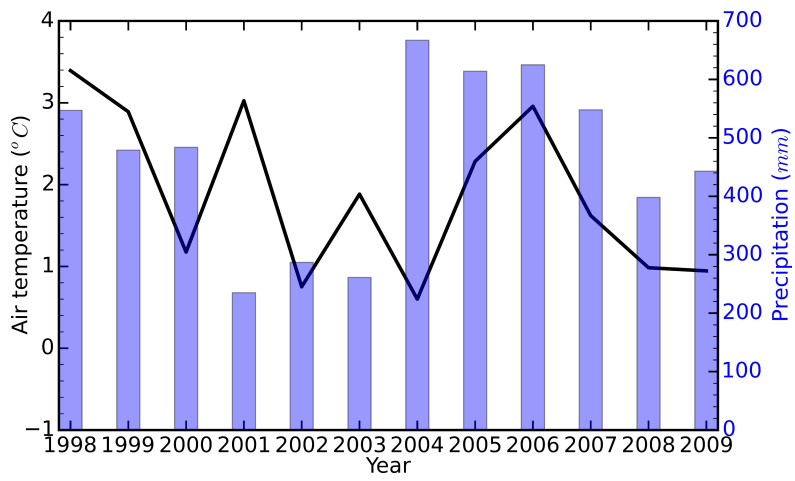
804



813

814 **Figure 1.** The location of the study site (Old Aspen Flux Tower)

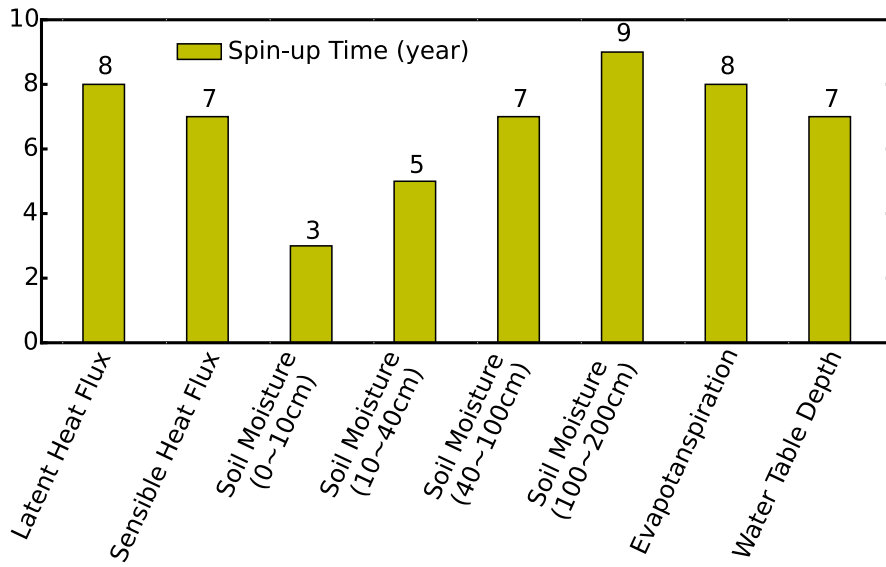
815



816

817 **Figure 2.** Monthly air temperature above canopy and precipitation at BERMS SK-OAS site

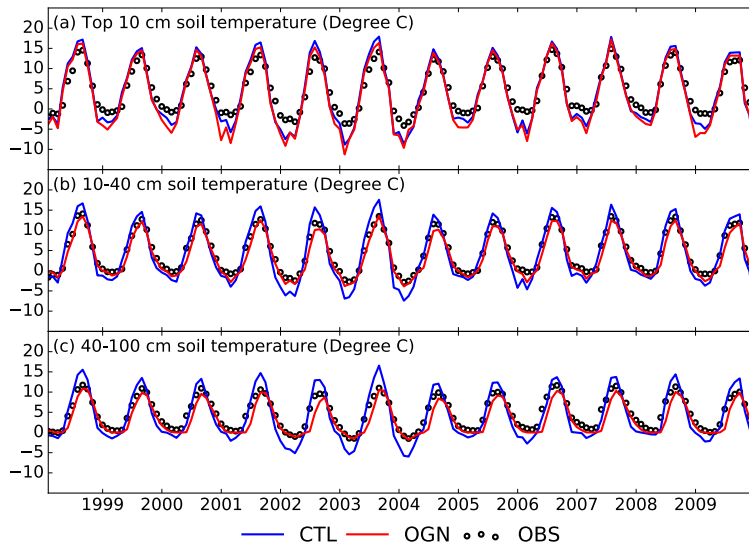
818



819

820 **Figure 3.** Averaged spin-up time (in years) for individual variables.

821

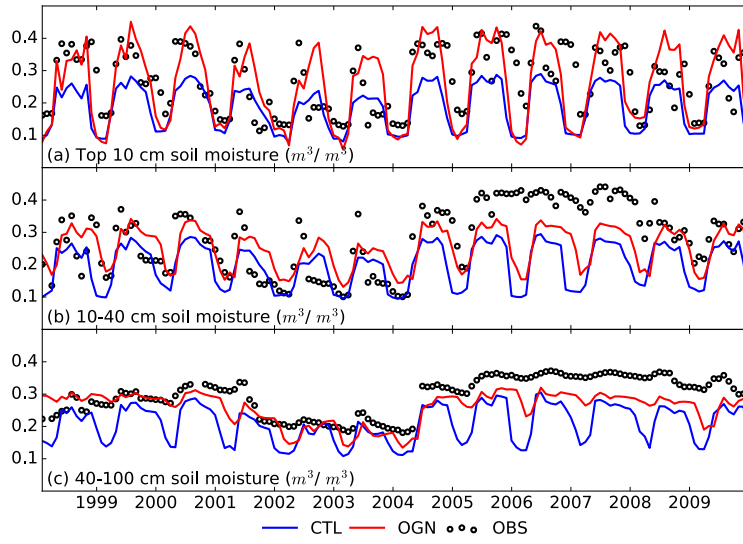


822

823 **Figure 4.** Observed and Noah-MP-simulated monthly soil temperature for BERMS SK-OAS site

824 at a depth of (a) top 10 cm, (b) 10-40 cm, and (c) 40-100 cm

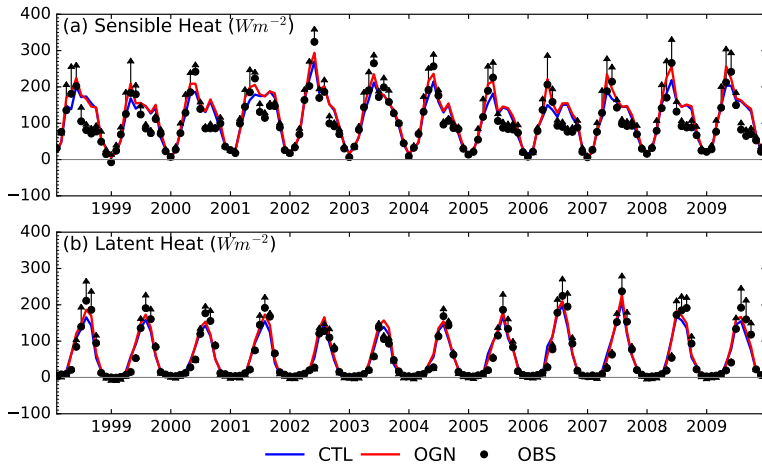
825



826

827 **Figure 5.** Observed and Noah-MP-simulated monthly soil moisture for BERMS SK-OAS site at  
 828 a depth of (a) top 10 cm, (b) 10-40 cm, and (c) 40-100 cm

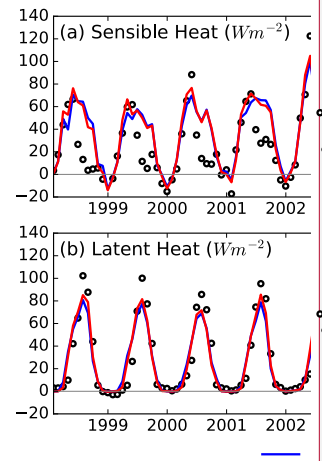
829



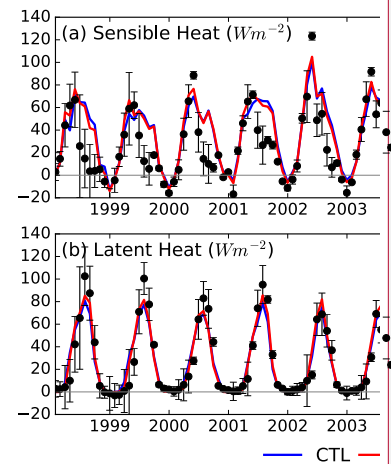
830

831 **Figure 6.** Observed and the Noah-MP simulated (CTL and OGN) daytime monthly-average,  
 832 sensible and latent heat flux above tree canopy. Error bars represent the average and deviations  
 833  $[(RN-G) \times B / (1+B)]$  for SH, and  $(RN-G) / (1+B)$  for LH] from observations, and B is the Bowen  
 834 ratio ( $B=SH/LH$ ).

835



Deleted:



Formatted: Font:Bold

Deleted:

Deleted: ,

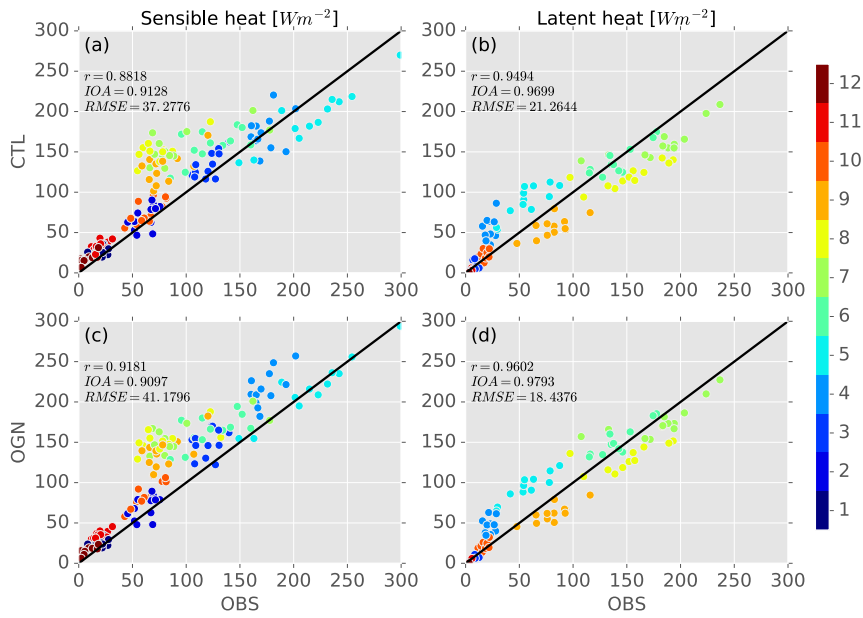
Deleted: *the e*

Deleted: *the*

Deleted:

Deleted: *data*

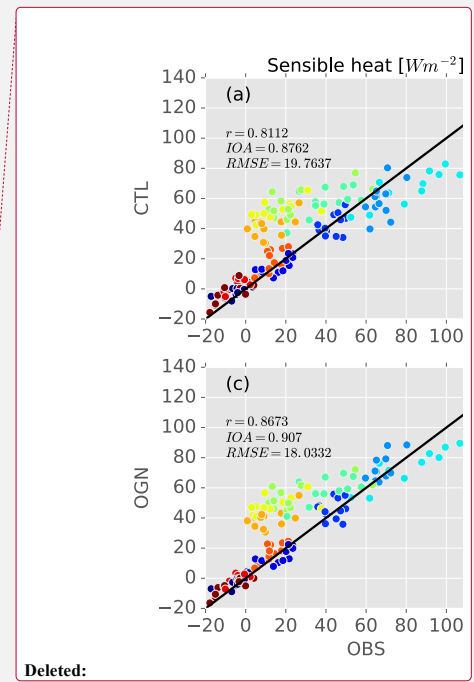
Deleted: the error bars represent the average and deviations (RN-SH-LH-G) from the observation data



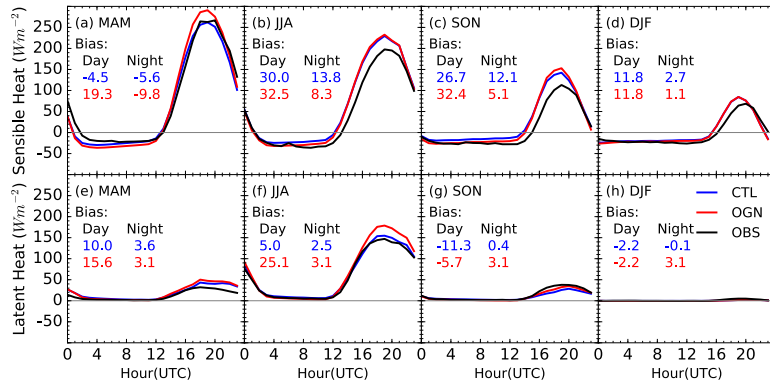
846

847 **Figure 7.** Scatterplots of the daytime monthly-averaged (a) sensible, (b) latent heat fluxes  
 848 ( $W m^{-2}$ ) for CTL versus the observation above canopy; the monthly-averaged (c) sensible, (d)  
 849 latent heat fluxes ( $W m^{-2}$ ) for OGN versus the observation above canopy. The color represents  
 850 each month from January (1) to December (12).

851



Deleted:

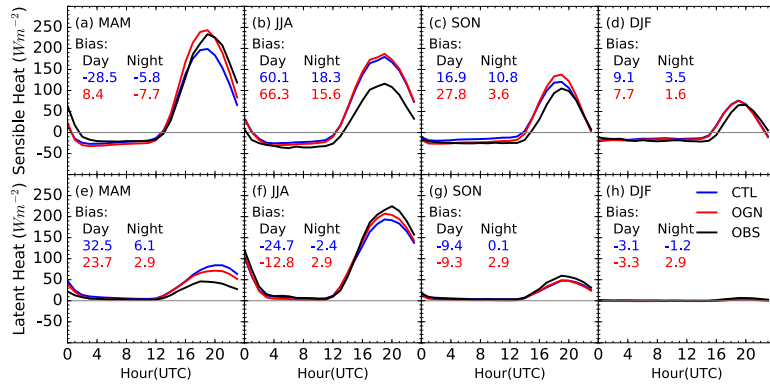


853

854 **Figure 8.** Comparison of the seasonal averaged diurnal cycle of the sensible and latent heat

855 fluxes at OAS site for drought years

856

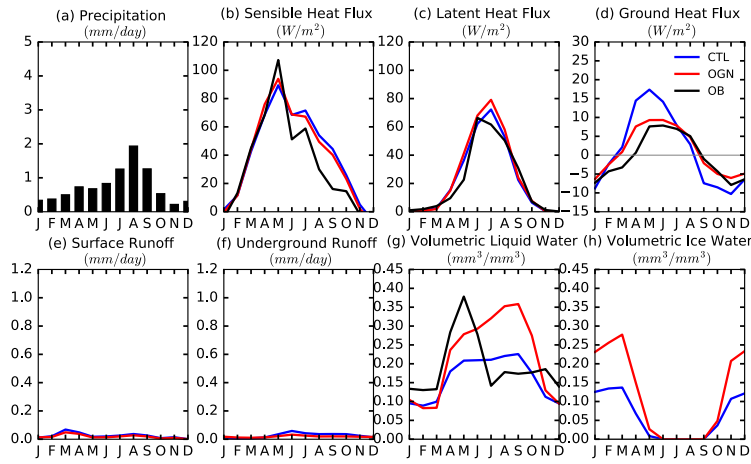


857

858 **Figure 9.** Comparison of the seasonal averaged diurnal cycle of the sensible and latent heat

859 fluxes at OAS site for wet years

860



861

862 **Figure 10.** Annual cycle of selected surface energy and hydrologic cycle fields for drought years.

863 Black line is the observation. Note that (a) is the observed precipitation, (b) is sensible heat flux,

864 (c) is latent heat flux, (d) is ground heat flux, (e) is surface runoff, (f) is underground runoff, (g)

865 is volumetric liquid water for soil layer one, (h) is volumetric ice water content for soil layer one.

866

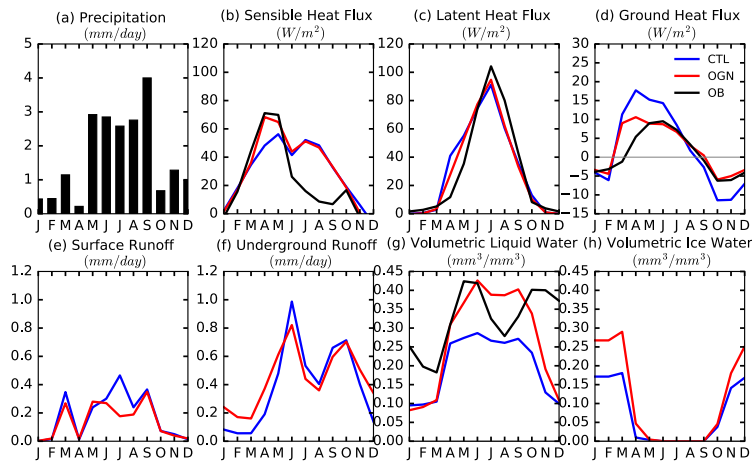
Deleted: Black line is the observation.

Deleted: the total column (1m depth) soil

Deleted: content changes

Deleted: the total column (1m depth) soil

Deleted: changes



872

873 **Figure 11.** Annual cycle of selected surface energy and hydrologic cycle fields for wet years.

874 Black line is the observation. Note that (a) is the observed precipitation, (b) is sensible heat flux,

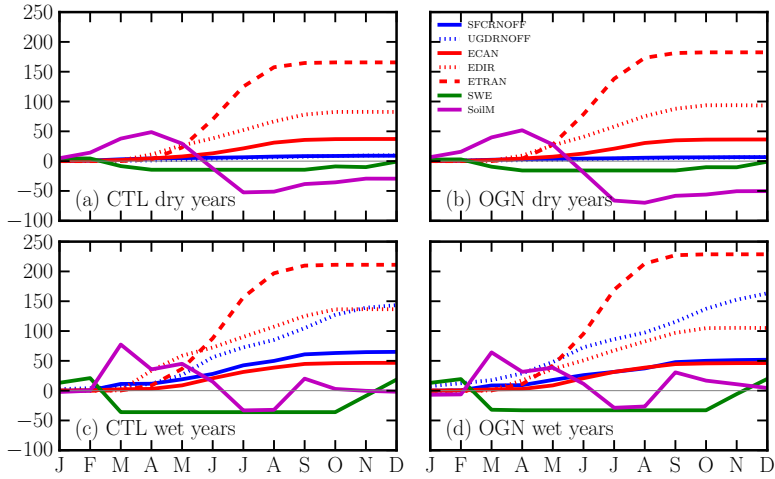
875 (c) is latent heat flux, (d) is ground heat flux, (e) is surface runoff, (f) is underground runoff, (g)

876 is volumetric liquid water content for soil layer one, (h) is volumetric ice water content for soil

877 layer one.

878

- Deleted: the total column (1m depth) soil
- Deleted: changes
- Deleted: the total column (1m depth) soil
- Deleted: changes



883

884 **Figure 12.** Water budgets: blue lines are accumulated surface runoff (mm), blue dots are  
 885 accumulated underground runoff (mm), red lines are accumulated evaporation of intercepted  
 886 water (mm), red dots are accumulated ground surface evaporation (mm), red dash lines are  
 887 accumulated transpiration (mm), green lines are snow water equivalent changes (mm), purple  
 888 lines are soil water content changes in the soil column (mm), (a) and (b) are averaged for 2002–  
 889 2003, (c) and (d) are averaged for 2005-2006.

The soil properties for each layer are specified as a weighted combination of organic and mineral soil properties.

$$P = (1 - f_{sc,i})P_m + f P_o \quad (2)$$

where  $P_m$  is the value for mineral soil,  $P_o$  is the value for organic soil, and  $P$  is the weighted average quantity.